



Pharmacotranscriptomic profiling of resistant triple-negative breast cancer cells treated with lapatinib and berberine shows upregulation of PI3K/Akt signaling under cytotoxic stress

Parham Jabbarzadeh Kaboli^{a,b,1,*}, Shuang Luo^{a,1}, Yao Chen^{a,c}, Masume Jomhori^d,
Saber Imani^e, Shixin Xiang^{a,c}, Zhigui Wu^{a,c,f}, Mingxing Li^{a,c}, Jing Shen^{a,c}, Yueshui Zhao^{a,c},
Xu Wu^{a,c}, Chi Hin Cho^{a,c}, Zhangang Xiao^{a,c,*}

^a Laboratory of Molecular Pharmacology, Department of Pharmacology, School of Pharmacy, Southwest Medical University, Luzhou 646000, Sichuan, PR China

^b Graduate Institute of Biomedical Sciences, Research Center for Cancer Biology, and Center for Molecular Medicine, China Medical University, Taichung, Taiwan, ROC

^c South Sichuan Institution for Translational Medicine, Luzhou 646000, Sichuan, PR China

^d Department of Biotechnology Research, Razi Vaccine and Serum Research Institute, Mashhad, Iran

^e Department of Oncology, The Affiliated Hospital of Southwest Medical University, Luzhou 646000, Sichuan, PR China

^f Department of Pharmacy, The Affiliated Hospital of Southwest Medical University, Luzhou 646000, Sichuan, PR China

ARTICLE INFO

Keywords:

Triple-negative breast cancer
Chemoresistance
Akt
PI3K
Lapatinib
Berberine

ABSTRACT

Triple-negative breast cancer (TNBC) is the most incurable type of breast cancer, accounting for 15–20% of breast cancer cases. Lapatinib is a dual tyrosine kinase inhibitor targeting EGFR and Her2, and berberine (BBR) is a plant-based alkaloid suggested to inhibit several cancer signaling pathways. We previously reported that lapatinib activates the Akt oncoprotein in MDA-MB231 TNBC cells. The present study determined the mechanism (s) of Akt activation in response to lapatinib, BBR, and capivasertib (Akt inhibitor) as well as the role of Akt signaling in chemoresistance in TNBC cells. Genetic profiles of 10 TNBC cell lines and patients were analyzed using datasets obtained from Gene Expression Omnibus and The Cancer Genome Atlas Database. Then, the effects of lapatinib, BBR, and capivasertib on treated MDA-MB231 and MCF-7 cell lines were studied using cytotoxicity, immunoblot, and RNA-sequencing analyses. For further confirmation, we also performed real-time PCR for genes associated with PI3K signaling. MDA-MB231 and MCF-7 cell lines were both strongly resistant to capivasertib largely due to significant Akt activation in both breast cancer cell lines, while lapatinib and BBR only enhanced Akt signaling in MDA-MB231 cells. Next-generation sequencing, functional enrichment analysis, and immunoblot revealed downregulation of CDK6 and DNMT1 in response to lapatinib and BBR lead to a decrease in cell proliferation. Expression of placental, fibroblast growth factor, and angiogenic biomarker genes, which are significantly associated with Akt activation and/or dormancy in breast cancer cells, was significantly upregulated in TNBC cells treated with lapatinib and BBR. Lapatinib and BBR activate Akt through upregulation of alternative signaling, which lead to chemoresistance in TNBC cell. In addition, lapatinib overexpresses genes related to PI3K signaling in resistant TNBC cell model.

1. Introduction

Triple-negative breast cancer (TNBC) tumors lack expression of estrogen receptors, progesterone receptors, and human epidermal growth factor receptors type 2 (Her2) and therefore, cannot be targeted by either Her2-targeted or hormone therapies. Among three major Asian ethnic groups (Chinese, Malay, and Indian), the TNBC subtype

accounted for 13% of all breast cancers (Thike et al., 2010). TNBC is the most aggressive subtype of breast cancer in which most deaths are due to poor chemotherapeutic response. Although systemic therapies, such as endocrine, targeted, and local (e.g., radio-embolization and microwave ablation), are used for TNBC, chemotherapy is still the main treatment. Tyrosine kinase, cyclin-dependent kinase (CDK)-4/6, and Poly (ADP-Ribose) Polymerase (PARP) inhibitors are the current chemotherapy of choice for TNBC (Costa et al., 2017; Beniey, 2019). For TNBC patients

* Corresponding authors.

E-mail addresses: dr.parham@mail.cmu.edu.tw (P. Jabbarzadeh Kaboli), xzg555898@hotmail.com (Z. Xiao).

¹ These authors contributed equally to this work.

<https://doi.org/10.1016/j.gene.2021.146171>

Received 6 June 2021; Received in revised form 5 December 2021; Accepted 13 December 2021

Available online 10 January 2022

0378-1119/© 2022 Elsevier B.V. All rights reserved.

Nomenclature			
Abbreviation	Full name		
TPM	transcripts per million kilobases	GEO	Gene Expression Omnibus
QNBC	Quadruple Negative Breast Cancers	ITGA7	Alpha-7 integrin
RB1	retinoblastoma protein-1	COL9A3	Collagen alpha-3(IX)
NFE2L2	Nuclear Factor, Erythroid 2 Like 2	IL6R	Interleukin 6 receptor
HDAC	Histone deacetylase	KITLG	Stem cell factor
CAP	Capivasertib	GNG3	G Protein Subunit Gamma 3
LAP	Lapatinib	GNG4	G Protein Subunit Gamma 4
RNASE	Ribonuclease	TEK	Angiopoietin-1 RTK
ANG	Angiogenin	EFNA2	Ephrin-A2
ANGPTL4	Angiopoietin-like 4	EFNA3	Ephrin-A3
PFKFB3	6-phosphofructo-2-kinase/fructose-2,6-biphosphatase 3	PGF	Placental growth factor
DNMT	DNA methyl transferase	FGF9	Fibroblast growth factor 9
CDK	Cyclin-dependent kinase	FGFR3	Fibroblast growth factor receptor 3
BBR	Berberine	PPP2R2B	Serine/threonine-protein phosphatase 2A regulatory subunit B beta
EGFR	Epidermal growth factor receptor	PDPK2P	Putative 3-phosphoinositide-dependent protein kinase 2
Her2	Human Epidermal growth factor receptor 2	PIK3R1	Phosphatidylinositol 3-kinase regulatory subunit alpha
TNBC	Triple-negative breast cancer	PIK3CB	Phosphatidylinositol-4,5-bisphosphate 3-kinase catalytic subunit beta
PD-L1	Programmed death-ligand 1	TNN	Tenascin N
RTK	Receptor tyrosine kinases	SHC4	Src Homology 2 Domain Containing Family, Member 4
GPCR	G-protein coupled receptors	RASGRP2	RAS guanyl-releasing protein 2
GSK	Glycogen synthase kinase	SYNGAP1	Synaptic KRAS GTPase-activating protein 1
MTT	3-(4,5-dimethyl-2-thiazolyl)-2,5-diphenyl-2H-tetrazolium bromide	PRKCG	Protein kinase C gamma type
DEGs	Differentially expressed genes	PLA2G4C	Phospholipase A2 Group IVC
KEGG	Kyoto Encyclopedia of Genes and Genomes	ETS2	ETS Proto-Oncogene 2
KOBAS	KO-Based Annotation System	CDKN1A	Cyclin-dependent kinase inhibitor 1
TCGA	The Cancer Genome Atlas	OSM	Oncostatin M
		BCL2L11	Bcl-2-like protein 11 (BIM)

expressing programmed death-ligand 1 (PD-L1), the monoclonal antibody atezolizumab which targets PD-L1 was recently approved for TNBC in combination with paclitaxel (Saleh et al., 2019); however, the TNBC indication of atezolizumab was withdrawn in August 2021. Chemoresistance is a major problem in TNBC treatment as the hypoxic tumor microenvironment is well-known to lead to chemoresistance (Saatci et al., 2020). Akt is a master regulator of hypoxic conditions by which generation of reactive oxygen species is regulated through activation of hypoxia-inducible factor-1 α , and therefore, the metabolism of breast cancer cells is remodeled (Jabbarzadeh Kaboli et al., 2020; Jabbarzadeh Kaboli, 2021).

Different types of receptors, including receptor tyrosine kinases (RTKs), cytokine receptors, G-protein coupled receptors (GPCRs), and integrin, are able to activate phosphoinositide-3-kinases (PI3K)/Akt signaling (Nitulescu et al., 2016). On the other hand, evidence implies that upregulation of KRAS is associated with resistance to epidermal growth factor receptor (EGFR/Her2)-targeted therapy. KRAS down-regulates EGFR downstream signaling, thereby decreasing EGFR sensitivity to EGFR inhibitors. Instead, overactivated KRAS activates Akt through activation of other RTKs (Young et al., 2013). Moreover, we recently found the EGFR/Her2 inhibitor lapatinib activates Akt in MDA-MB231 TNBC cells but not in MCF-7 breast cancer cells (Jabbarzadeh Kaboli et al., 2019; Jabbarzadeh Kaboli and Ling, 2020). In addition, it is well-established that the herbal alkaloid berberine (BBR) can be used as an inhibitor of cancer growth and metastasis. BBR targets several cancer signaling pathways in breast cancer cells, including mitogen-activated protein kinase (MAPK), PI3K/Akt, and hedgehog (Jabbarzadeh Kaboli et al., 2014; Kaboli et al., 2017). Here, for the first time, a prospective *in vitro* investigation was conducted to determine the mechanism(s) of Akt activation in response to lapatinib, BBR, and capivasertib (an Akt inhibitor). Furthermore, we sought to explore the role of Akt signaling in TNBC chemoresistance, with particular focus on oncogenic networks

within TNBC cells.

2. Methods

2.1. Chemicals and reagents

Lapatinib [Cat no. 231277922; MedChemExpress, NJ, USA], BBR [Cat no. 633658; MedChemExpress], and capivasertib [Cat no. 1143532391; MedChemExpress] were dissolved in dimethyl sulfoxide [Cat no. 67685; Sigma-Aldrich, St. Louis, MO, USA]. 3-(4,5-dimethyl-2-thiazolyl)-2,5-diphenyl-2H-tetrazolium bromide [MTT; Tocris Bioscience, UK] was used to assess cell death. Primary rabbit antibodies p-Akt (Ser473) [Cat no. 9271S], Akt [Cat no. 9272S], CDK6 [Cat no. 1331T], CDK4 [Cat no. 12790S], p-glycogen synthase kinase (GSK)-3 α/β (Ser9) [Cat no. 5558S], DNA methyl transferase (DNMT)-1 [Cat no. 5119S], multidrug resistance protein-1 [Cat no. 12273S], GSK-3 α/β [Cat no. 5676], and β -actin [Cat no. 4970S] were purchased from Cell Signaling Technology (MA, USA), while EGFR [Cat no. ET1603-37] and p-EGFR (Y1068) [Cat no. ET1612-30] primary antibodies were purchased from Huabio (China). The dilution ratios of all primary antibodies were 1:1000. The Dye-free Chemiluminescence Imaging system and ClarityTM Western ECL substrate [Cat no. 1705061] were obtained from Bio-Rad Laboratories Inc. (Hercules, CA, USA). Immobilon-P polyvinylidene fluoride membranes [Cat no. IPVH00010] and PhosSTOP [Cat no. 4906845001] were purchased from Sigma-Aldrich, while RIPA lysis buffer [Cat no. R0010] came from Solarbio Life Sciences (Beijing, China).

To extract RNA and to perform quantitative reverse transcriptase polymerase chain reaction (qRT-PCR) we purchased Trizol reagent [Cat no. 260710, Ambion, Austin, TX, USA], DEPC Water [Cat no. R0022, Beyotime Institute of Biotechnology, Shanghai, China], Ethanol [Cat no. CAS64175, Cologne Chemical Company Ltd., Germany], Isopropyl

alcohol [Cat no. CAS67630, Cologne Chemical Company Ltd., Germany], FastKing RT Kit [Cat no. KR116-2, Tiangen Biotech, Beijing, China], and 2x TSINGKE Master qPCR Mix (SYBR Green I) [Cat no. TSE201, TsingKe, China]. To run qPCR, we also used T100™ Thermal Cycler [Cat no. 1861096, Bio-Rad Laboratories, Inc.] and CFX Connect™ Optics Module [Cat no. 1855201, Bio-Rad Laboratories, Inc.] instruments. Primer sequences were as follows:

GAPDH-F: 5' - CTGGGCTACACTGAGCACC – 3'
GAPDH-R: 5' - AAGTGGTCGTTGAGGGCAATG – 3'
AKT1-F: 5' - AGCGACGTGGCTATTGTGAAG – 3'
AKT1-R: 5' - GCCATCATTCTTGAGGAGGAAG T – 3'
GSK3B-F: 5' - AGACGCTCCCTGTGATTTATGT – 3'
GSK3B-R: 5' - CCGATGGCAGATTCCAAAGG – 3'
PTEN-F: 5' - TGGATTGCACTTAGACTTGACCT – 3'
PTEN-R: 5' - GGTGGGTTATGGTCTTCAAAGG – 3'
MYC-F: 5' - GTCAAGAGCGAACACACAAC – 3'
MYC-R: 5' - TTGGACGGACAGGATGTATGC – 3'
PIK3R1-F: 5' - ACCACTACCGGAATGAATCTCT – 3'
PIK3R1-R: 5' - GGGATGTGCGGGTATATCTTC – 3'
PIK3CA-F: 5' - CCACGACCATCATCAGGTGAA – 3'
PIK3CA-R: 5' - CCTCACGGAGGCATTCTAAAGT – 3'

2.2. Cell culture

The non-metastatic breast cancer cell line MCF-7 and metastatic breast cancer cell line MDA-MB231 were purchased from American Type Culture Collection (Manassas, VA, USA). MDA-MB231 cells were grown in 25-cm² flasks with Dulbecco's Modified Eagle's Medium (Thermo Fisher Scientific, Waltham, MA, USA), and MCF-7 cells were cultured in 25-cm² flasks with RPMI-1640 (Thermo Fisher Scientific). Both cell lines were supplemented with 10% fetal bovine serum (Gibco, Thermo Fisher) and 1% penicillin-streptomycin-glutamine (Sigma-Aldrich).

2.3. Cytotoxic assay

BBR and lapatinib cytotoxicity was estimated using an MTT assay (Abcam, Shanghai, China), following the manufacturer's directions. In brief, MDA-MB231 and MCF-7 cells were cultured in 96-well microplates (3000 cells/well for 24 h); four wells were used for each concentration. Cells were then treated with serial concentrations of BBR (0, 2, 5, 15, 25, or 50 μM), lapatinib (0, 2, 5, 15, 25, or 50 μM), and/or capivasertib (0, 0.2, 0.4, 0.8, 1.5, or 2.5 μM) for different time periods (24, 48, or 72 h). After incubating with MTT, the absorbance was measured at 570 nm using a porous microplate detection system (Gene Company Ltd., Beijing, China). Experiments were performed in triplicate, and data were presented as the mean of three independent experiments.

2.4. Protein extraction and western blotting

To detect protein levels, Western blotting was performed. Total cellular protein was extracted in ice-cold RIPA lysis buffer supplemented with PhosSTOP. Then, equal amounts of protein (30 μg of whole cell lysate per lane) were separated via 7.5% or 10% sodium dodecyl sulfate-polyacrylamide gel electrophoresis and transferred onto Immobilon polyvinylidene fluoride membranes. Membranes were treated with p-Akt, Akt, CDK4, CDK6, p-GSK-3β, GSK-3α/β, DNMT1, multidrug resistance protein-1, and β-actin primary antibodies overnight at 4 °C. After washing the membranes three times with phosphate-buffered saline (PBS)-Tween buffer, membranes were incubated with the appropriate horseradish peroxidase-based anti-rabbit immunoglobulin G secondary antibody (1:2000) for 1 h at room temperature. Finally, proteins were visualized using Clarity™ Western ECL substrate via Dye-free Chemiluminescence Imaging System. Immunoblot analysis was done in duplicate for each treated and negative control samples.

2.5. RNA extraction

Total RNA was extracted from MDA-MB231 cells using TRIzol® Reagent according to the manufacturer's instructions (Invitrogen, Carlsbad, CA, USA), and genomic DNA was removed using DNase I (TaKaRa Bio Inc., Mountain View, CA, USA). Then, RNA quality was determined by 2100 Bioanalyzer (Agilent Technologies, Santa Clara, CA, USA) and quantified using the ND-2000. To extract total RNA, four groups of cells (A–D) were prepared in duplicate: A1 and A2 were treated with 50 μM lapatinib, B1 and B2 were treated with 50 μM BBR, C1 and C2 were treated with 25 μM lapatinib plus 25 μM BBR, and D1 and D2 were negative controls.

2.6. Library preparation and sequencing

An RNA-sequencing (RNA-seq) transcriptome library was prepared with a TruSeq™ RNA sample preparation kit (Illumina Inc., San Diego, CA, USA) using 1 μg of total RNA. mRNA was isolated according to a polyA selection method by oligo(dT) beads and then fragmented by fragmentation buffer. Then, double-stranded cDNA was synthesized using a SuperScript double-stranded cDNA synthesis kit (Invitrogen) with random hexamer primers (Illumina Inc.). The synthesized cDNA was subjected to end-repair, phosphorylation, and "A" base addition according to Illumina's library construction protocol. Libraries were size selected for cDNA target fragments of 200–300 bp on 2% Low Range Ultra Agarose followed by PCR amplification using Phusion DNA polymerase (NEB) for 15 PCR cycles. After quantifying by TBS380, a paired-end RNA-seq sequencing library was sequenced with the Illumina HiSeq xten/NovaSeq 6000 sequencer (2 × 150 bp read length; Illumina Inc.) at the BCM-FGI core, following the manufacturer's protocols.

2.7. Read mapping

Raw paired-end reads were trimmed and quality controlled by Seq-Prep (<https://github.com/jstjohn/SeqPrep>) and Sickle (<https://github.com/najoshi/sickle>) with default parameters. Clean reads were separately aligned to the reference genome with orientation mode using TopHat software version 2.0.0 (<http://tophat.cbcb.umd.edu/>) (Trapnell et al., 2009). The mapping criteria of bowtie were as follows: sequencing reads should be uniquely matched to the genome allowing up to 2 mismatches, without insertions or deletions. Then, the gene region was expanded following depths of sites to obtain the operon. In addition, the whole genome was split into multiple 15-kbp windows that share 5 kbp. New transcribed regions were defined as more than 2 consecutive windows without overlapped gene regions, where at least 2 reads were mapped per window in the same orientation.

2.8. Differential expression and functional enrichment

To identify differentially expressed genes (DEGs) between samples, the expression level of each transcript was calculated according to the fragments per kilobase of exon per million mapped reads method. RSEM (<http://deweylab.biostat.wisc.edu/rsem/>) (Li and Dewey, 2011) was used to quantify gene abundances. R statistical package software EdgeR (<http://www.bioconductor.org/packages/2.12/bioc/html/edgeR.html>) (Robinson et al., 2010) was utilized for DEG analysis. In addition, functional-enrichment analysis including gene ontology and Kyoto Encyclopedia of Genes and Genomes (KEGG) analysis were performed to identify which DEGs were significantly enriched in gene ontology terms and metabolic pathways at a Bonferroni-corrected $P \leq 0.05$ compared with the whole transcriptome background. Gene ontology functional enrichment and KEGG pathway analysis were carried out by Goatools (<https://github.com/tanghaibao/Goatools>) and KO-Based Annotation System (KOBAS) (<http://kobas.cbi.pku.edu.cn/home.do>) (Xie et al., 2011).

2.9. New isoform prediction

The TopHat-Cufflinks pipeline was used to predict gene isoforms from RNA-seq data. In TopHat version 2.0.0 (<http://tophat.cbcb.umd.edu/>) (Trapnell et al., 2009), the expected fragment length was set to 200-bp, and the “small-anchor-fraction” was set to 0.08, which requires at least 8-bp on each side of an exon junction for the 100-bp RNA-seq data. Cuffcompare was used to compare and merge the reference annotation and isoform predictions.

2.10. Alternative splice event identification

All alternative splice events that occurred were identified by using the recently released program Multivariate Analysis of Transcript Splicing (<http://rnaseq-mats.sourceforge.net/>) (Shen et al., 2012). Only the isoforms that were similar to the reference or were comprised of novel splice junctions were considered, and splicing differences were detected as exon inclusion, exclusion, alternative 5', 3', and intron retention events.

2.11. The cancer genome atlas (TCGA) and gene expression omnibus (GEO) analysis

In order to compare gene expression between different TNBC cell lines, expression data was obtained from GSE36133 and GSE36139 GEO datasets (<https://pubmed.ncbi.nlm.nih.gov/>). As the GSE36133 and GSE36139 data were from different platforms, they were combined by batch effect. Then, the expression of 38 genes in 10 TNBC cell lines was compared as well as the expression of each gene in different cell lines. In addition, the expression of the same genes in clinical data obtained from TCGA database was compared. After downloading the data from TCGA (<http://cancergenome.nih.gov>), it was normalized according to our previous article (Zhao et al., 2019). The normalized expression of RNA sequences (transcripts per million kilobases, TPM) contained 113 normal samples and 115 TNBC tumor patients. To understand the effects of androgen signaling in TNBC cells, gene expression in quadruple-negative breast cancer (QNBC) cells was also analyzed. Low expression of the androgen receptor gene was defined as negative by quartile method to obtain QNBC data. The QNBC data was first normalized then log2 transformed. The normalized expression of RNA sequence (TPM) for QNBC contained 113 normal samples and 96 QNBC tumor patients.

2.12. Quantitative RT-PCR

Use FastKing RT Kit (with gDNase), first configure the gDNA removal reaction system in Table 1, mixed thoroughly, centrifugation briefly, incubated for 3 min at 42 °C in T100™ Thermal Cycler. Using 2xTSINGKE Master qPCR Mix (SYBR Green I), qPCR reaction system, and qPCR reaction program, CFX Connect™ Optics Module, the expression level was determined using the $2^{-\Delta\Delta Ct}$ method. To conduct qRT-PCR, we designed each experiments in triplicates for MDA-MB231 and MCF-7 cell lines (with three dependent and three independent samples).

2.13. Statistical analysis

All statistical analyses were performed using SPSS software version 21.0 (SPSS Inc., Chicago, IL, USA) with an unpaired Student's *t*-test unless otherwise stated. All graphs were produced by GraphPad Prism 5.0 for Windows (GraphPad Software Inc., La Jolla, CA, USA). Two-tailed *t*-tests were also performed, and a **P* < 0.05, ***P* < 0.01, and ****P* < 0.001 were considered significant.

Table 1

Key genes upregulated in MDA-MB231 cells treated with lapatinib and BBR. Key upregulated genes can be categorized in seven groups: (1) cytokine receptors, (2) cell–cell/matrix receptors, (3) Phosphoinositide 3-kinase regulators, (4) G protein-coupled receptors, (5) receptor tyrosine kinases and growth factors, (6) KRAS activators, and (7) tumor suppressors.

Gene	Full name	Regulation	Function
<i>ITGA7</i>	Alpha-7 integrin	Up	Cell migration process
<i>COL9A3</i>	Collagen alpha-3(IX)	Up	Pathogenesis of breast cancer
<i>IL6R</i>	Interleukin 6 receptor	Up	Promote breast cancer stem cell feature
<i>KITLG</i>	Stem cell factor	Up	Promotes phosphorylation of PIK3R1/GPCR signaling
<i>GNG3</i>	G Protein Subunit Gamma 3	Up	GPCR/Calcium signaling
<i>GNG4</i>	G Protein Subunit Gamma 4	Up	GPCR/Calcium signaling
<i>TEK</i>	Angiopoietin-1 RTK	Up	Angiogenesis and cell migration
<i>EFNA2</i>	Ephrin-A2	Up	Cell-cell interaction
<i>EFNA3</i>	Ephrin-A3	Up	Cell-cell interaction
<i>PGF</i>	Placental growth factor	Up	Angiogenesis
<i>FGF9</i>	Fibroblast growth factor 9	Up	Tumor growth and invasion
<i>FGFR3</i>	Fibroblast growth factor receptor 3	Up	Cancer cell proliferation, survival, and migration
<i>PPP2R2B</i>	Serine/threonine-protein phosphatase 2A regulatory subunit B beta	Up	Negative control of cell growth
<i>PDPK2P</i>	Putative 3-phosphoinositide-dependent protein kinase 2	Up	Akt, PKA, and PKC-ζ signaling pathways
<i>PIK3R1</i>	Phosphatidylinositol 3-kinase regulatory subunit alpha	Up	PI3K/Akt signaling
<i>PIK3CB</i>	Phosphatidylinositol-4,5-bisphosphate 3-kinase catalytic subunit beta	Up	PI3K/Akt signaling
<i>TNN</i>	Tenascin N	Up	Angiogenesis and migration
<i>SHC4</i>	Src Homology 2 Domain Containing Family, Member 4	Up	KRAS activation
<i>RASGRP2</i>	RAS guanyl-releasing protein 2	Up	KRAS activation
<i>SYNGAP1</i>	Synaptic KRAS GTPase-activating protein 1	Up	KRAS regulation
<i>PRKCG</i>	Protein kinase C gamma type	Up	PKC signaling
<i>PLA2G4C</i>	Phospholipase A2 Group IVC	Up	Inflammation and the immune response
<i>ETS2</i>	ETS Proto-Oncogene 2, Transcription Factor	Up	Proto-oncogene transcription factor
<i>CDKN1A</i>	Cyclin-dependent kinase inhibitor 1	Up	Tumor suppressor p21
<i>OSM</i>	Oncostatin M	Up	Growth negative regulator
<i>BCL2L11</i>	Bcl-2-like protein 11 (BIM)	Up	Pro-apoptotic protein

Red: Upregulation of oncoproteins involved in metastasis, angiogenesis, and cell migration. Green: Upregulation of tumor suppressors.

3. Results

3.1. Transcriptional profile of TNBC cell lines and patients

3.1.1. Tumor suppressors PTEN and RB1 downregulation promote tumorigenesis in TNBC cell lines

To determine the mechanism(s) of chemoresistance in TNBC, genes related to tumor suppressors, Akt signaling, and epigenetic regulation were listed and then their transcription analyzed in 10 TNBC cell lines (Fig. 1) as well as TNBC and QNBC patients (Fig. 2). We observed that tumorigenesis in TNBC cell lines may be less dependent on EGFR

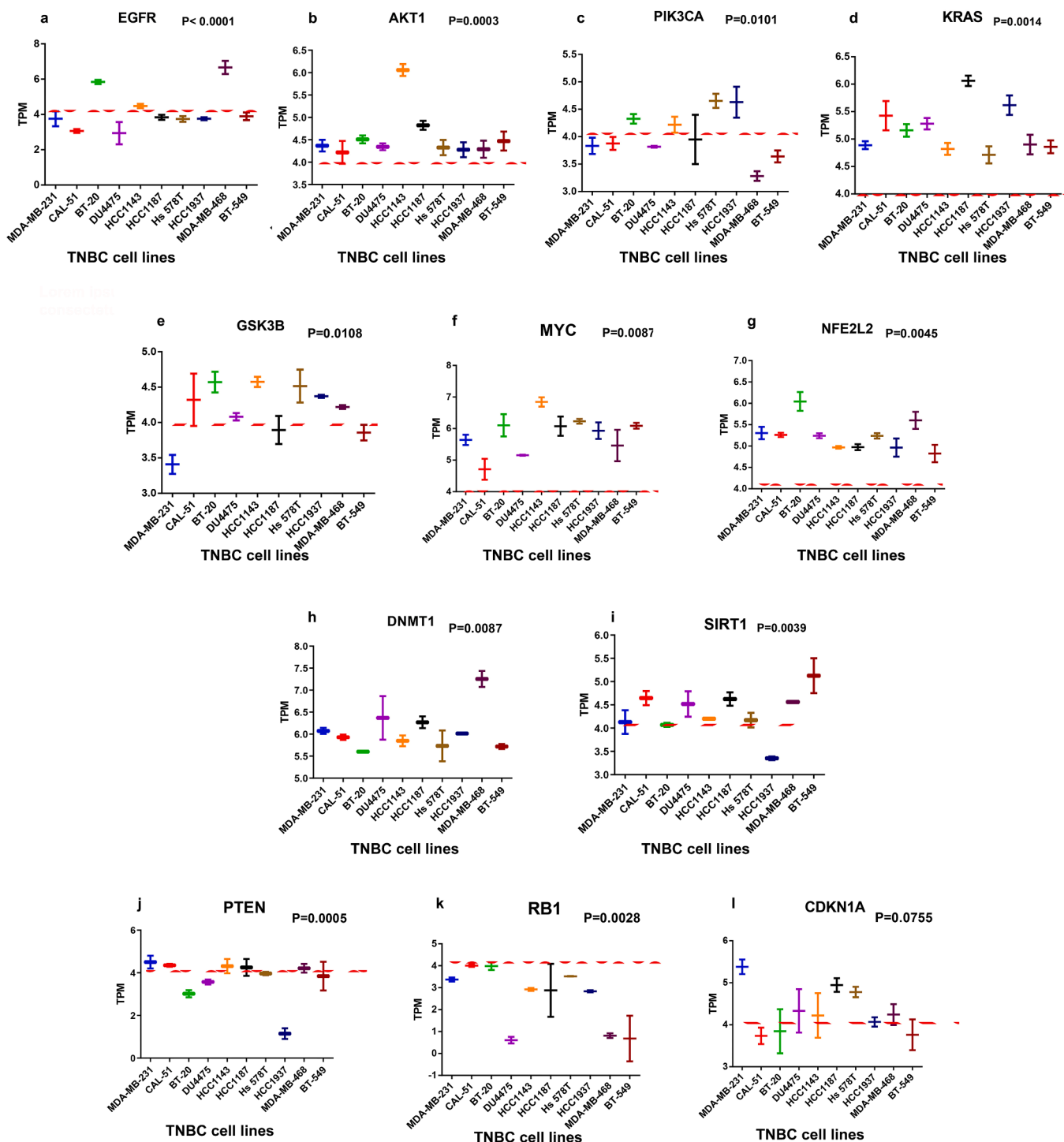


Fig. 1. Expression of different oncogenic proteins associated with Akt in 10 TNBC cell lines. (a-g) PI3K/Akt signaling proteins; (h-i) Epigenetic regulators; (j-l) Tumor suppressors. Expression data obtained from GSE36133 and GSE36139 in the GEO database. The expression of *PIK3CA*, *AKT1*, and *EGFR* in MDA-MB231 cells is relatively low compared with other TNBC cells. Instead, *PTEN*, which inhibits PI3K/Akt signaling, is higher in MDA-MB231 cells. The horizontal line is a threshold above which is considered high expression. *DNMT1* has high expression in TNBC cell lines, suggesting its positive effects in cell cycle regulation; MDA-MB468 cells had the highest *DNMT1* expression.

(Fig. 1a); however, *KRAS* has a crucial role on TNBC proliferation and tumorigenesis because it triggers PI3K/Akt signaling EGFR-independently and MAPK/BRAF signaling EGFR-dependently (Fig. 1d). On the other hand, *AKT1* expression is remarkably increased in HCC1143 and HCC1187 cells, which may be due to PI3K/Akt crosstalk with other signaling proteins such as GSK-3 β , Myc and Nrf2 (Fig. 1e, f, g). The analysis of TNBC cell lines revealed a dramatic drop in

phosphatase and tensin homolog (*PTEN*) expression in HCC1937, BT-20, and DU4475 cells, while other cell lines had almost a basic level of *PTEN* expression (Fig. 1j). *PTEN* suppresses tumor cell growth and proliferation through inhibition of PI3K/Akt signaling (Fig. 1c). As *PTEN* is basically expressed in most TNBC cells (except HCC1937, BT-20, and DU4475), PI3K/Akt signaling is decreased in most TNBC cells, though not zero. Therefore, a decrease in phosphatidylinositol-4,5-

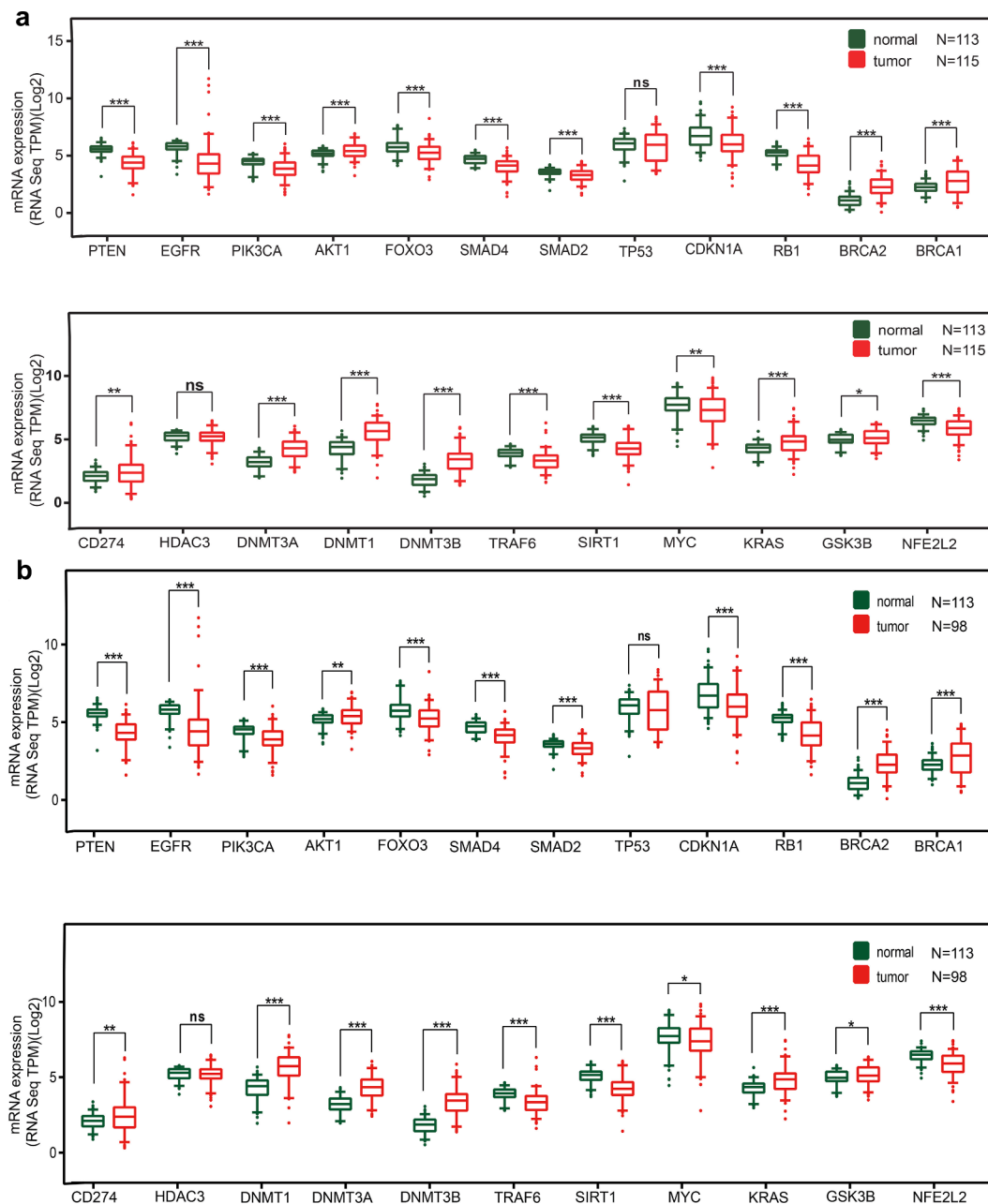


Fig. 2. Expression of different oncogenic genes associated with Akt in TNBC and QNBC patients versus normal patients. Expression data obtained from TCGA database: (a) TNBC; (b) QNBC. Expression of *DNMT1*, *DNMT3A*, and *DNMT3B* (epigenetic regulators) as well as *AKT1* and *KRAS* (oncoproteins) was upregulated in TNBC and QNBC patients, while *EGFR* was downregulated, suggesting Akt and KRAS pathways can be upregulated in an EGFR-independent manner.

bisphosphate-3-kinase catalytic subunit α (*PIK3CA*) gene expression rationally decreases Akt activation. In addition, the retinoblastoma protein-1 gene (*RB1*) is downregulated in all TNBC cells lines, leading to a remarkable increase in tumor cell proliferation (Fig. 1k). RB1 is a crucial tumor suppressor in TNBC cells whose expression is also remarkably decreased in TNBC and QNBC patients. In contrast, *TP53* expression did not show any significant difference between TNBC and normal patients (Fig. 2).

3.1.2. KRAS, MYC, and PI3K/Akt signaling upregulation enhance cell cycle in TNBC cell lines

Furthermore, since Akt plays a crucial role in chemoresistance in TNBC cells, the expression of *AKT1*, *EGFR*, *PIK3CA*, *KRAS*, *GSK3B*, *MYC*, and nuclear factor erythroid 2-related factor 2 (*NFE2L2*) genes were assessed in the 10 TNBC cell lines (Fig. 1). *AKT1* expression had medium

activity in almost all TNBC cell lines with a TPM of around 4–4.5, except for HCC1143 cells, which had remarkable upregulation of *AKT1*, with a TPM of more than 6 (Fig. 1b). *PIK3CA* transcription was decreased in HCC1143 cells but overexpressed in HCC1937 cells, while *PTEN* was specifically downregulated. Therefore, higher *AKT1* expression in HCC1143 cells may be due to the activity of other signaling proteins, such as Myc and KRAS, both of which are strongly expressed in TNBC cells, specifically in HCC1143, which had the highest *MYC* expression; however, *KRAS* expression was the highest in HCC1187 and HCC1937 cells. On the other hand, *AKT1* and *KRAS* expression were both increased in HCC1187 cells.

3.1.3. Akt regulation in TNBC cell lines and patients may be EGFR-independent

Data obtained from TNBC and QNBC patients revealed that *PTEN*

expression is significantly decreased in both TNBC ($N = 115$) and QNBC ($N = 98$) patients (Fig. 2). Analysis of clinical data from TNBC and QNBC patients showed the average expression of *PIK3CA* was lower than that in normal patients, but the transcriptional levels of *AKT1* were higher than *PIK3CA* (p110 alpha gene) in both normal and TNBC/QNBC patients. As p110 alpha is upstream from Akt activation, the activation of Akt in TNBC and QNBC patients seems to be p110 alpha-independent, at least to some extent. *KRAS* was remarkably upregulated in both TNBC and QNBC patients. On the other hand, *EGFR*, which expresses a receptor tyrosine kinase directly associated with PI3K/Akt signaling, was downregulated in most TNBC cell lines, except MDA-MB468 and BT-20, as well as TNBC patients. In addition, *NFE2L2*, which is involved in the upregulation of proteins associated with anti-oxidant signaling and multidrug resistance, was upregulated in all TNBC cell lines, with MDA-MB468 and BT-20 having the highest levels. However, *NFE2L2* expression in clinical TNBC samples was lower than that in the normal group, which needs further investigation.

3.1.4. Epigenetic regulators DNMTs, but not HDACs, are upregulated in TNBC cell lines and patients

In order to explore the roles of epigenetic regulation in TNBC cells, expression of histone deacetylase (*HDAC3*, *HDAC8*, *HDAC9*, and *SIRT1*) and DNA methyl transferase (*DNMT1*, *DNMT3A*, and *DNMT3B*) genes was assessed in the 10 TNBC cell lines. The *DNMTs* and *SIRT1* were found to be significantly upregulated in all TNBC cell lines (Fig. 1h-i). In

fact, *DNMT1* expression was overexpressed in all TNBC cells, with the highest expression in MDA-MB468 cells. In contrast, *SIRT1* expression was lower, with the lowest expression in HCC1937 cells and the highest in BT-549 cells. Having compared the DNMT expressions in TNBC cell lines (Fig. 1h) and TNBC patients (Fig. 2), we found DNMT upregulation may have a crucial role in tumorigenesis of TNBC. Using *in vitro* study, we later confirmed that DNMT1 is associated with CDK6 upregulation.

3.2. Drug treatment and *in vitro* study

3.2.1. Lapatinib and BBR, but not capivasertib, decreased cell cycles in both TNBC and *Her2*⁺ cell lines by more than 50%

MTT assay was used to study the effects of lapatinib, BBR, and capivasertib on MDA-MB231 and MCF-7 cell survival (Fig. 3). The effects of BBR on both cell lines were time dependent, and the half maximal inhibitory concentrations (IC_{50}) of 72 h BBR treatment were 15 and 20 μM for MDA-MB231 and MCF-7 cells, respectively; the IC_{50} s for BBR reached around 40 μM after 24 and 48 h (Fig. 3a-b). In contrast, both cell lines were more sensitive to lapatinib. In addition, MCF-7 cells showed reduced survival in response to lapatinib and had a higher IC_{50} compared to MDA-MB231 cells. The number of live MCF-7 cells after 24 h treatment with low concentrations of lapatinib dramatically dropped, whereas the number of MDA-MB231 cells rose initially then dropped when the treatment was extended to 48 and 72 h (Fig. 3c-d). The IC_{50} s of lapatinib significantly decreased in both cell lines compared with BBR,

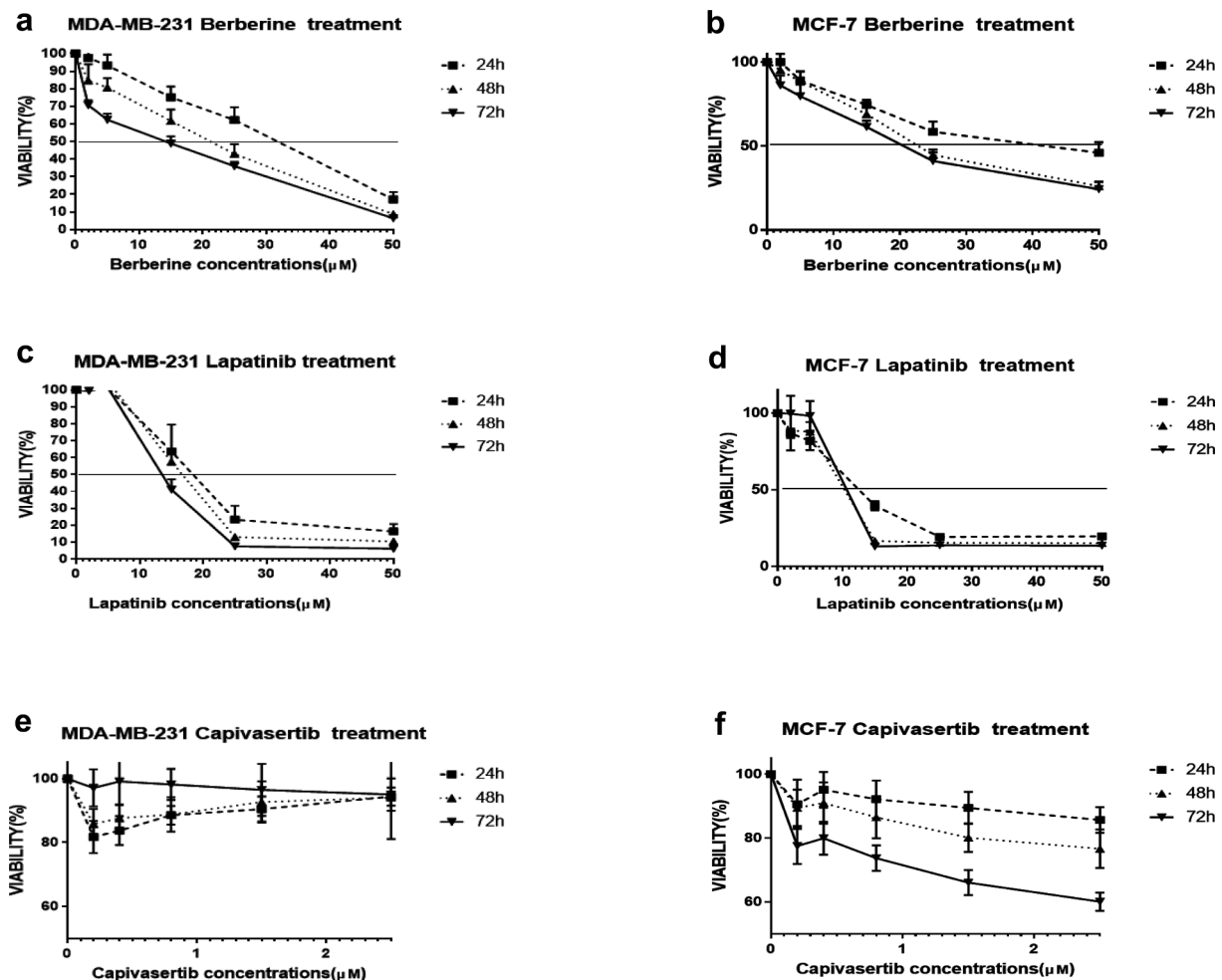


Fig. 3. Viability of MDA-MB231 and MCF cells in response to chemotherapy. (a-b) BBR-treated MDA-MB231 (a) and MCF-7 (b) cells; (c-d) lapatinib-treated MDA-MB231 (c) and MCF-7 (d) cells; (e-f) capivasertib-treated MDA-MB231 (e) and MCF-7 (f) cells. Although MDA-MB231 and MCF cells showed higher number of dead cells in response to lapatinib and BBR, neither cell line responded to capivasertib at all. However, cells considered dead due to lapatinib and/or BBR treatment may need further investigation to determine whether they are truly dead or dormant.

especially after 48 and 72 h treatments. Surprisingly, both cell lines were strongly resistant to capivasertib and their survival rates were not affected by capivasertib. Therefore, we were not able to estimate IC₅₀s for the different capivasertib treatments (Fig. 3e–f).

3.2.2. Lapatinib and BBR toxic stress decreased CDK6 and DNMT1 levels in both cell lines, but enhanced Akt phosphorylation in TNBC cells

To study the effects of BBR and lapatinib on the mechanisms of chemoresistance in MDA-MB231 cells, we first detected the levels of p-Akt, CDK4, and CDK6 proteins in response to 5 and 25 μM lapatinib and BBR after 48 h (Fig. 4). These results will determine whether the higher amounts of dead cells estimated in cytotoxicity assays were dead or dormant, a state in which cell signaling is being reprogrammed. While 25 μM BBR and lapatinib treatment (toxic stress) activated Akt in MDA-MB231 cells (Fig. 4a–b), demonstrating that higher concentrations reversed the effects of these compounds on Akt activation. CDK6 levels were decreased with both low and high drug concentrations, confirming the reduction in MDA-MB231 cell proliferation observed in cytotoxicity assays (Fig. 4a–b).

3.2.2.1. Capivasertib increased CDK6, DNMT1, and p-Akt levels in both TNBC and Her2 cell lines. Based on cytotoxicity assay and immunoblot, capivasertib poorly affected cell cycles of MDA-MB231 and MCF-7 cell lines. Surprisingly, capivasertib, a known Akt inhibitor, strongly activated Akt in MDA-MB231 and MCF-7 cells. In contrast to BBR and lapatinib, capivasertib activated Akt at concentrations as low as 0.8 μM. However, the mechanism of capivasertib activation of Akt is likely different from that of BBR and lapatinib because CDK6 and DNMT1 levels were increased in capivasertib-treated MDA-MB231 cells (Fig. 4a–b) (Figure S1). In addition, p-Akt levels were inhibited in response to 25 μM BBR and lapatinib. In fact, toxic stress due to high concentrations of BBR and lapatinib did not activate Akt in MCF-7 cells. However, p-Akt was increased in response to capivasertib in MCF-7 cells (Fig. 4c–d).

3.2.2.2. Genes involved in PI3K and KRAS pathways are affected in TNBC cells treated with lapatinib and BBR. To study the effects of lapatinib and BBR on the transcriptome and understand gene expression under toxic conditions, whole-genome RNA-seq was used twice for each treated and negative control groups. Therefore, MDA-MB231 cells were separately treated with 50 μM of lapatinib and BBR as well as with a combination of 25 μM lapatinib plus 25 μM BBR (Fig. 5). PBS-treated groups were used as negative controls. KEGG enrichment analysis showed three intracellular pathways, including MAPK, PI3K/Akt, and KRAS, as well as cytokine-cytokine receptor genes were at the top of the list. Seventy-three, 72, and 49 genes associated with PI3K/Akt, MAPK, and KRAS pathways, respectively, were found to be targeted by lapatinib, whereas 59, 54, and 28 genes, respectively, were targeted by BBR (Fig. 5a, b, c). The number of genes targeted by combination treatment was fewer than with either monotherapy. Thirty genes associated with the PI3K/Akt pathway were common between the two monotherapies and combination treatment, whereas the number of genes associated with KRAS signaling that were common in the three treatment groups changed into 16 (Fig. 5c). According to DEG analysis (Fig. 5d–e), 26 key genes associated with PI3K/Akt signaling were upregulated in response to individual lapatinib and BBR treatments, most of which are involved in tumor progression, cell–cell interactions, and cell migration (Table 1) (Fig. 5f). Hence, the function of each upregulated gene in PI3K/Akt and KRAS pathways was examined further, as they may be a reason for the unexpected Akt activation in response to lapatinib and BBR reported above. RNA-seq results are presented in Table S1.

3.2.2.3. Transcriptomic analysis shows a reduced rate of cell cycle is accompanied by tumorigenesis in TNBC cells treated with lapatinib and BBR. Having compared genes targeted by lapatinib (A groups) and BBR (B groups) with controls (D groups), we found that several genes associated with tumorigenesis were upregulated (Figs. 6 and 7). In addition, upregulation of tumor suppressor [e.g., p21 (CDKN1A) and Ser/Threonine phosphatase 2A 55 kDa regulatory subunit B β isoform

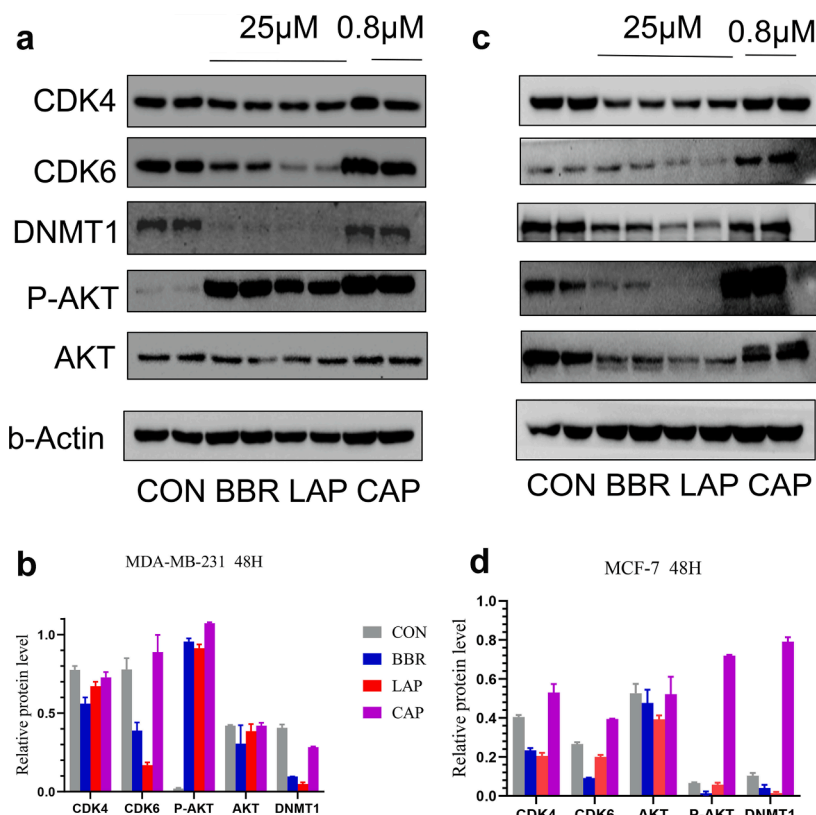


Fig. 4. Immunoblot analysis after 48-h treatment. (a–b) MDA-MB231 cells. Lapatinib and BBR increased p-Akt levels and, in contrast, decreased CDK6 and DNMT1, which confirm cell cycle is arrested while Akt signaling is activated in TNBC cells. (c–d) MCF-7 cells. p-Akt levels is decreased after lapatinib and BBR treatment. Both cell lines showed significant resistance to capivasertib, and p-Akt levels as well as CDK6/DNMT1 were strongly increased in response to capivasertib in MCF-7 cells. Each result obtained two dependent (extracted from the same flask) and two independent (extracted from different flask) repeats. CON: negative controls; BBR: berberine; LAP: lapatinib; CAP: capivasertib.

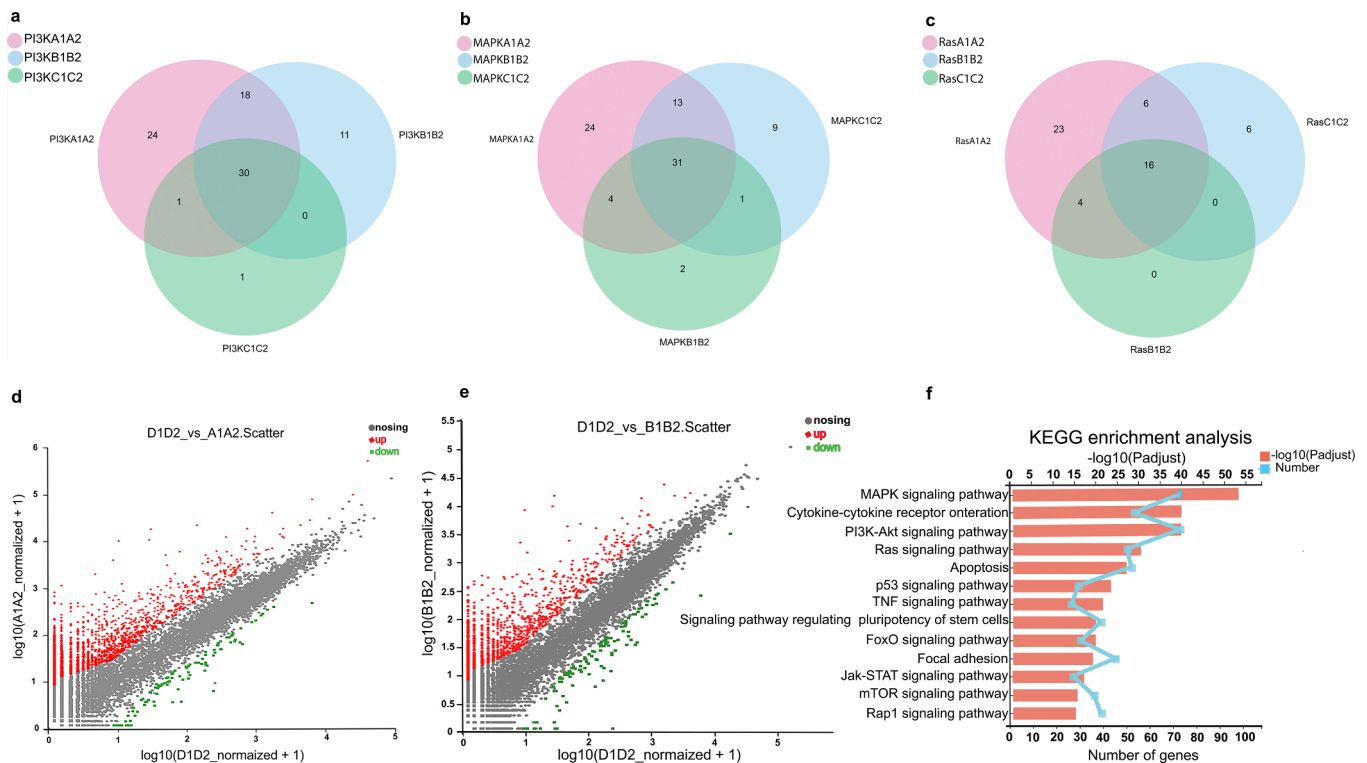


Fig. 5. Next-generation sequencing analysis of MDA-MB231 cells treated with lapatinib and BBR. (a–c) The number of genes associated with (a) PI3K/Akt, (b) MAPK, and (c) Ras signaling targeted by lapatinib, BBR, and lapatinib plus BBR. (d–e) DEGs of controls versus samples treated with (d) lapatinib or (e) BBR. (f) KEGG enrichment analysis. PI3K/Akt, MAPK, KRAS, and cytokine pathways are located at the top of pathways targeted by lapatinib. Experiments were performed twice for each sample. D1D2: negative controls; A1A2: lapatinib-treated cells; B1B2: BBR-treated cells; C1C2: lapatinib plus BBR-treated cells.

(*PPP2R2B*), pro-apoptotic [*BCL2*-like 11], RTK [e.g., fibroblast growth factor (FGF) receptor 3 (*FGFR3*)], and growth factor [e.g., *FGF9* and placental growth factor (*PGF*)] genes as well as genes whose protein products are mainly involved in *PIK3CA* regulation [e.g., PI3K regulatory subunit 1 (*PIK3R1*) and 3-phosphoinositide-dependent protein kinase 2 (*PDPK2P*)], cell–cell interaction and migration [e.g., integrin subunit α 7, ephrin A2 (*EFNA2*), collagen type IX α 3 chain (*COL9A3*), and tenascin N (*TNN*)], breast cancer stem cell maintenance [interleukin (IL)-6 receptor], and G-protein signaling that regulates intracellular calcium levels (e.g., G-protein subunit γ 3 and KIT ligand) could all lead to remodeling of MDA-MB231 cell signaling in response to lapatinib and BBR (Fig. 6a).

Moreover, lapatinib plus BBR treatment reversed the separate effects of gene upregulation associated with each monotherapy. Many genes which were upregulated with lapatinib or BBR alone were downregulated when these drugs were combined. For example, *IL6R*, *TNN*, and *FGFR3* were downregulated with lapatinib plus BBR. Pathway analysis showed that crucial proteins located upstream of the PI3K/Akt pathway, such as RTKs, growth factors, cytokines, cytokine receptors, and GPCRs, were upregulated after combination treatment. Direct regulators of PI3K/Akt signaling, such as *PIK3R1* and *PDK1*, were also upregulated with combination treatment of MDA-MB231 cells (Fig. 6b).

3.2.2.4. Genes related to PI3K pathway are upregulated in MDA-MB231 cells treated with lapatinib. We previously showed that Akt is phosphorylated after treatment with lapatinib and BBR. In addition, our transcriptomic analysis showed that PI3K signaling and mTOR signaling are overexpressed in lapatinib- and BBR-treated MDA-MB231 cells. To confirm our transcriptomic data, we performed qRT-PCR for *PIK3CA*, *PIK3R1*, *Akt1*, *GSK3 β* , *PTEN*, and *Myc* in triplicates before and after treatment with lapatinib and BBR in MDA-MB231 and MCF-7 cell lines (Fig. 7). We observed that PI3K signaling is greatly upregulated in MDA-MB231 cells compared with MCF-7 cells. We also observed that both

compounds (lapatinib and BBR) can overexpress PI3K signaling; however, lapatinib upregulated *Myc* greater than BBR. Moreover, we found that *PIK3CA* is dramatically overexpressed in both MDA-MB231 and MCF-7 cells. These experiments indicated PI3KCA-dependent genes (e.g., *PIK3R1*, *Akt1*, *GSK3 β*) are overexpressed in resistant MDA-MB231 cells; however, the activation of these proteins is highly dependent on other factors such as other pathways cross talking with Akt in response to hypoxic condition.

3.2.2.5. KRAS GTPase regulators and growth factors are upregulated in TNBC cells treated with lapatinib and BBR. KRAS signaling was also upregulated with lapatinib and BBR monotherapy (Fig. 8). While *EGFR* was downregulated in MDA-MB231 cells treated with lapatinib or BBR, RTK-related genes, such as *FGFR3*, *TEK*, and *EFNA2/3*, were upregulated, which activates KRAS and PI3K/Akt signaling pathways. Although *FGF5* was downregulated, other growth factor genes whose products activate RTK signaling, such as *PGF* and *FGF9*, were upregulated. On the other hand, adaptors of KRAS, such as SHC adaptor protein 4 (*SHC4*), RAS guanyl releasing protein 2 (*RASGRP2*), and synaptic RAS GTPase activating protein 1 (*SYNGAP1*), were upregulated after treatment with lapatinib and BBR, leading to KRAS signal regulation in MDA-MB231 cells. As KRAS signaling crosstalks with PI3K/Akt signaling, upregulation of KRAS may be another important reason for the unexpected activation of Akt upon exposure to chemotherapy.

Collectively, our results showed that MDA-MB231 cells treated with lapatinib and BBR showed *PIK3CB*, *PIK3R1*, and *PIK3R3* upregulation, which leads to Akt activation through activation of *PIK3CA* (Fig. 9). Simultaneously, FGF and FGFR genes as well as KRAS activators (guanine nucleotide exchange factors and GTPase-activating proteins) were upregulated in MDA-MB231 cells treated with lapatinib and BBR, which altogether may lead to the observed chemoresistance to lapatinib and, to a lesser extent, BBR. Furthermore, chemotherapeutic treatment of MDA-MB231 cells showed that calcium signaling was also activated. Pathway

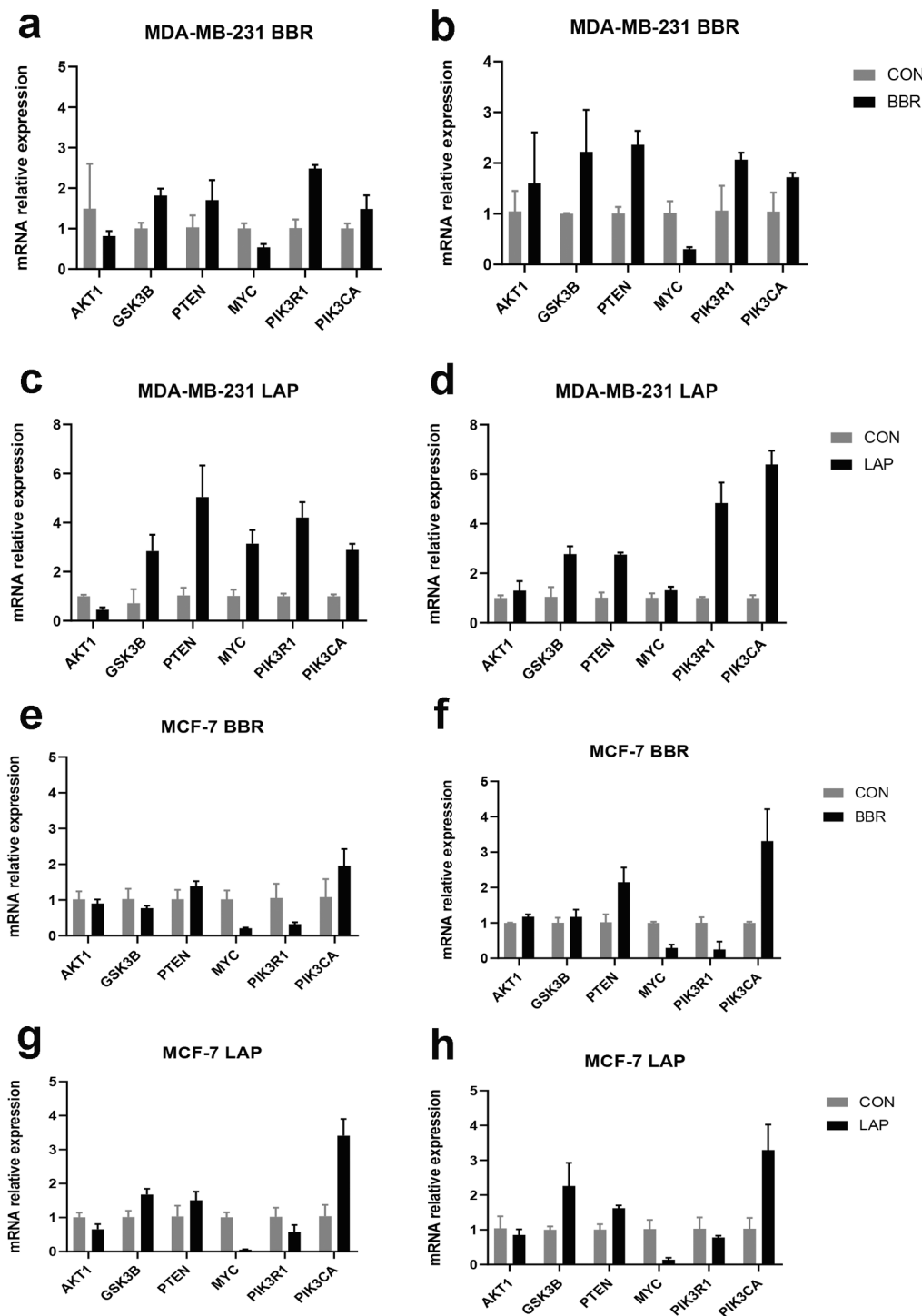


Fig. 7. Expression of key genes related to PI3K signaling using quantitative RT-PCR. (a-b) MDA-MB231 cells treated with BBR, (c-d) MDA-MB231 cells treated with lapatinib (LAP), (e-f) MCF-7 cells treated with BBR, (g-h) MCF-7 cells treated with lapatinib; *PIK3CA* is overexpressed in all treated cells; however, *PIK3R1*, *PTEN*, and *GSK3B* are overexpressed in treated MDA-MB231 cells. Three samples were used for each measurement using $2^{-\Delta\Delta Ct}$ method. CON: negative controls; BBR: berberine (25 μ M); LAP: lapatinib (25 μ M).

analysis of lapatinib-treated cells revealed chemoresistance in MDA-MB231 cells under toxic conditions. Lapatinib and BBR both upregulated *KRAS* and *PI3K/Akt* pathways, and cell proliferation was simultaneously decreased due to *CDK6* downregulation and *CDKN1A* upregulation. In addition, calcium is required for cellular movement and migration, and calcium signaling was activated through GPCRs and protein kinase C (*PKC*) upregulation, which leads to remodeling of cell

signaling and further metastasis and invasiveness. Survival analysis of gene candidates from TNBC cell lines treated with lapatinib and compared TCGA data showed that these genes should be considered when developing targeted therapies to overcome chemoresistance in TNBC. Finally, of the upregulated gene candidates in TNBC patients obtained from transcriptomic analysis, *PGF* has the highest hazard ratio (Fig. 10).

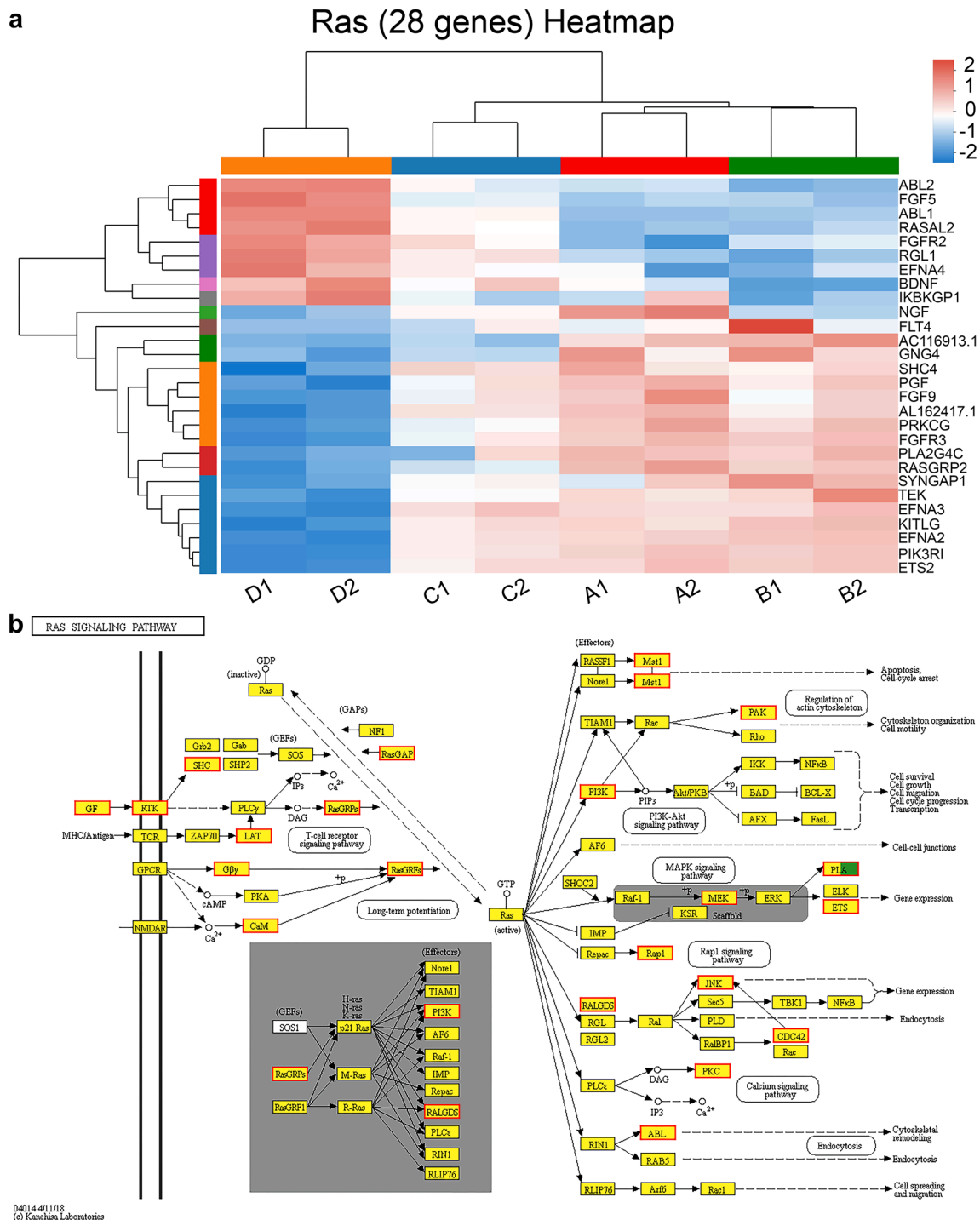


Fig. 8. Effects of lapatinib and BBR on gene expression, and KRAS pathway analysis of MDA-MB231 cells. (a) Heatmap of KRAS signaling showing up- and downregulated genes in A1A2, B1B2, and C1C2 samples. Genes involved in RTK signaling (e.g., *FGFR3*, *FGF9*, *PGF*, *TEK*, etc.) and KRAS activation [e.g., RAS guanyl releasing protein 2 (*RASGRP2*) and synaptic RAS GTPase activating protein 1 (*SYNGAP1*)] were upregulated by lapatinib and BBR. (b) KRAS pathway analysis shows KRAS upregulation by lapatinib and BBR, leading to upregulation of calcium signaling and crosstalk with Akt signaling. Ward’s algorithm with Euclidean distance metric was used as clustering method. www.majorbio.com web-based tool was used to build heatmap. Experiments were performed twice for each sample. **D1D2:** negative controls; **A1A2:** lapatinib-treated cells; **B1B2:** BBR-treated cells; **C1C2:** lapatinib plus BBR-treated cells.

4. Discussion

In the present study, gene expression of selected oncoproteins was studied in 10 TNBC cell lines and TNBC patients using data obtained from GEO and TCGA databases. The current findings highlighted that most chosen cell lines, including MDA-MB231, and TNBC patients have downregulated *AKT1*, *PIK3CA*, *PTEN*, and *EGFR* as well as upregulated

KRAS and *DNMTs*, suggesting they are associated with TNBC invasiveness. Furthermore, immunoblot analysis showed Akt activation is low in PBS-treated MDA-MB231 and MCF-7 cells. However, treating them with lapatinib strongly activated Akt in MDA-MB231 but not MCF-7 cells, indicating different reaction mechanisms to lapatinib. This result is in consistent with our previous report (Jabbarzadeh Kaboli and Ling, 2020).

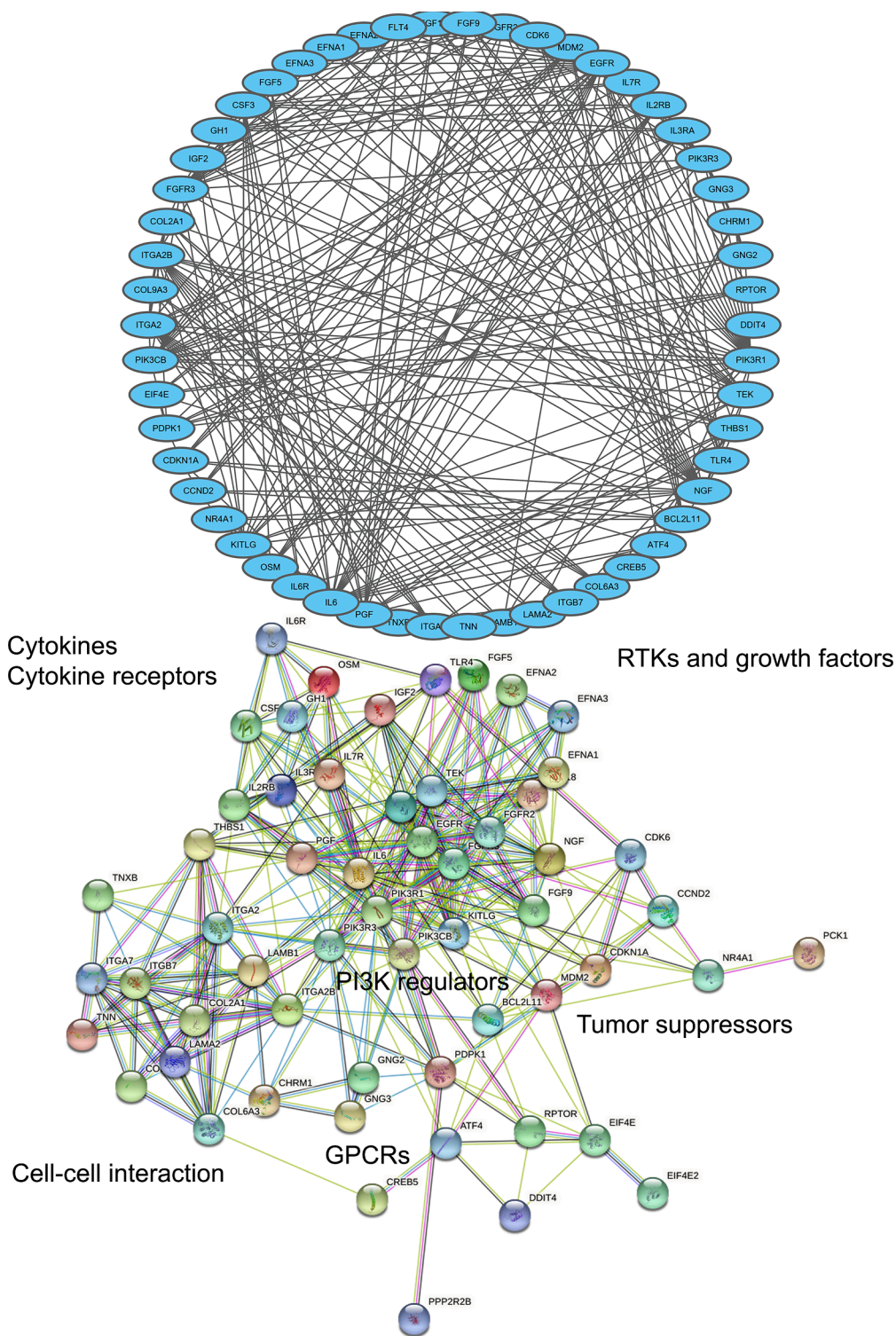


Fig. 9. Network analysis of PI3K/Akt signaling. Key genes affected by lapatinib and BBR belong to: (1) cytokine receptors, (2) cell–cell/matrix receptors, (3) PI3K regulators, (4) G protein-coupled receptors, (5) RTKs and growth factors, and (6) tumor suppressors. CDK6 downregulation and p21 gene (*CDKN1A*) were upregulated to reduce cell proliferation. In contrast, several genes, including *PGF*, *FGFR3*, *FGF9*, *PDPK1*, *IL6R*, and integrin subunit $\alpha 7$ (*ITGA7*) were upregulated, which lead to activation of alternative oncogenic signaling.

As mentioned earlier, KRAS overactivation desensitizes EGFR, resulting in resistance to EGFR-targeted therapies. Alternatively, other RTKs affected by overactivated KRAS lead to Akt upregulation (Young et al., 2013). As EGFR is downregulated in MDA-MB231 cells, Akt should be activated by other RTKs. The resistance to lapatinib is already known to be associated with alteration of the phosphoproteome, and related remodeling performed in the kinetome may lead to the poor response to lapatinib in breast cancer. Reactivation of PI3K/Akt signaling is also associated with loss of sensitivity to lapatinib in breast cancer. It was

previously shown that Akt can be activated in an EGFR-independent manner by the RTK AXL (Ruprecht et al., 2017). Additionally, mechanistic target of rapamycin complex 2 activation may activate Akt through crosstalk with other pathways (Werfel et al., 2018; van der Noord et al., 2019). PI3K/Akt activation has been reported in cisplatin-resistant MDA-MB231 cells as well (Gohr et al., 2017). Altogether, these results indicate that Akt signaling is a master switch of chemoresistance in TNBC cells (Fig. 11).

On the other hand, the association of epigenetic regulators with

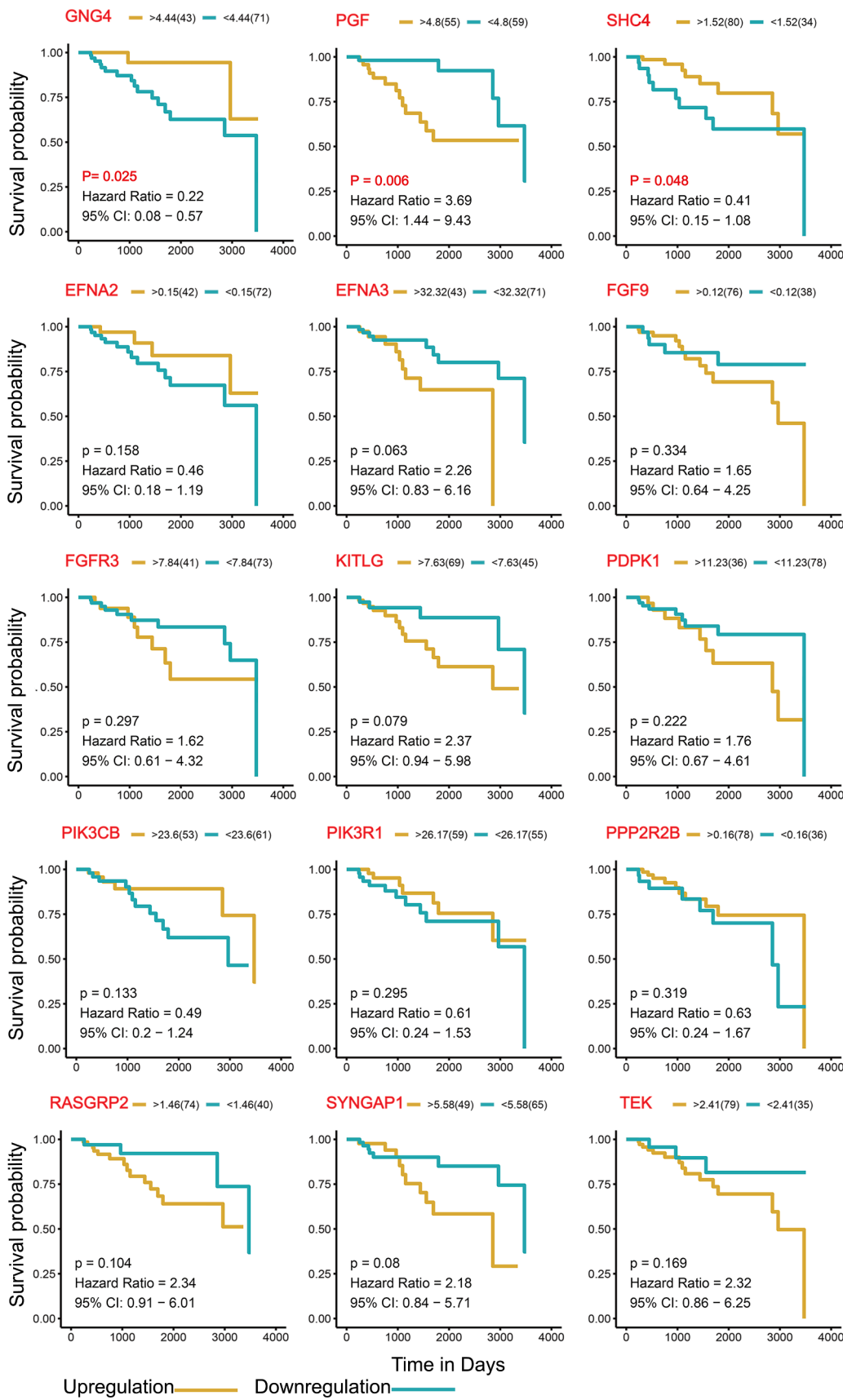


Fig. 10. Survival analysis and hazard ratios of final gene candidates. Genes upregulated in lapatinib-treated MDA-MB231 cells were compared with clinical TCGA data to show their importance in the survival of TNBC patients. PlGF, a growth factor involved in angiogenesis and produced by PGF, had the highest hazard ratio among the other proteins. Genes, such as KIT ligand (*KITLG*) and synaptic RAS GTPase activating protein 1 (*SYNGAP1*), and their products should be also considered in future studies.

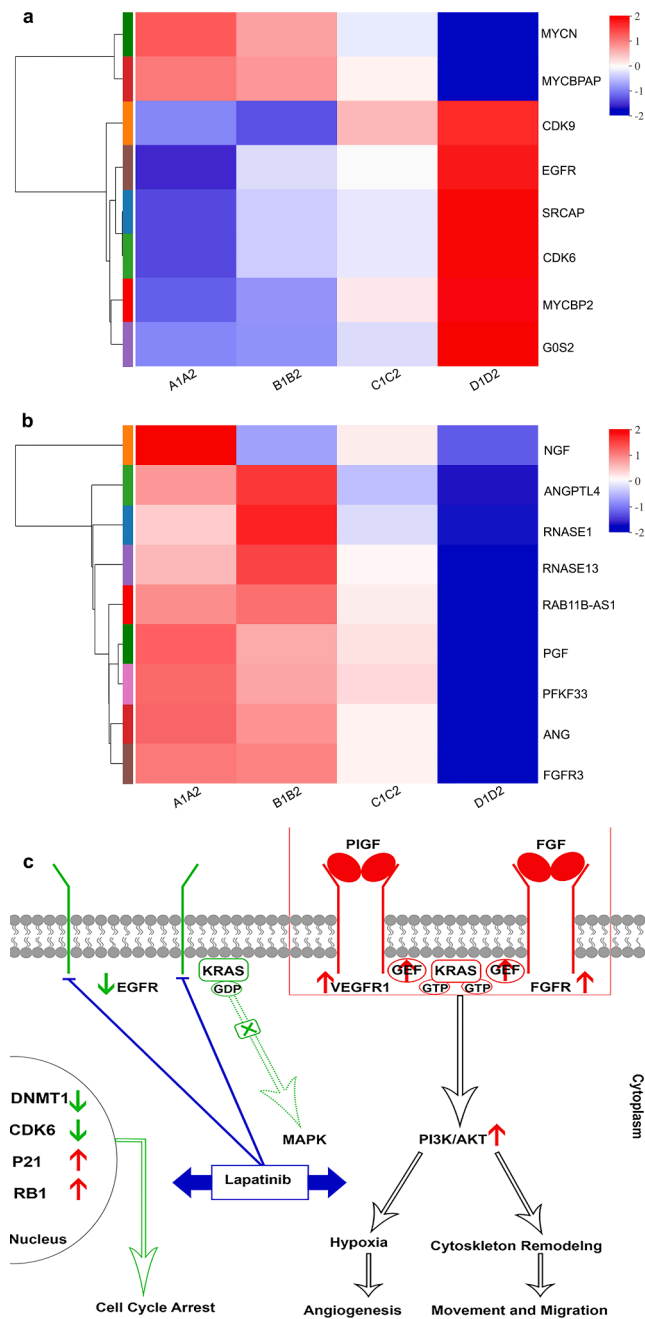


Fig. 11. A model for cellular defense against lapatinib chemotoxicity in TNBC. Lapatinib results in a dormancy/stem cell-like stage through which oncogenic pathways are reprogrammed by first, cell cycle downregulation and then, PI3K/Akt pathway upregulation in an EGFR-independent manner. **(a)** Effects of lapatinib and BBR on genes mainly regulate cell cycle in MDA-MB231 cells. EGFR and cyclin-dependent kinases CDK6 and 9 as well as Myc- and Src- associated proteins are downregulated in TNBC cells. Instead, MYCN, which is reported a few cancers including neuroblastoma was upregulated in lapatinib treatment. **(b)** Effects of lapatinib and BBR on biomarker genes mainly regulate angiogenesis in MDA-MB231 cells. Growth factors such as NGF and PGF as well as angiogenic biomarkers including ANG, ANGPTL4, RAB11B-AS, and PFKFB3 were upregulated in lapatinib and BBR treatments. **(c)** Model of resistance to lapatinib in MDA-MB231 cells. This model suggests lapatinib has a potential to enhance aggressiveness of TNBC cells by upregulating alternative growth factors and pro-inflammatory cytokines secreted in the tumor microenvironment. However, this model needs further elucidation to determine and validate tissues/organs where reprogrammed TNBC cells tend to migrate (e.g., brain, bones, etc.). Experiments were performed twice for each sample. **D1D2:** negative controls; **A1A2:** lapatinib-treated cells; **B1B2:** BBR-treated cells; **C1C2:** lapatinib plus BBR-treated cells. **G0S2:** G0/G1 switch gene 2; **NGF:** nerve growth factor; **ANGPTL4:** angiopoietin-like 4; **RAB11B-AS:** RAB 11B antisense RNA 1; **RNASE:** ribonuclease; **ANG:** angiogenin/RNASE5; **PFKFB3:** 6-phosphofructo-2-kinase 3; **PIGF:** placental growth factor; **FGF:** fibroblast growth factor; **VEGFR1:** Vascular Endothelial Growth Factor Receptor 1; **GEF:** Guanine nucleotide exchange factors (e.g., RASGRP2).

CDKs including *CDK6* and *CDK9* has been already reported, affecting the response of cancer cells to EGFR-targeted therapy (Bourdeau and Ferbeyre, 2016; McLaughlin et al., 2019; Zhang et al., 2018). Therefore, both CDK and DNMT inhibitors reduce proliferation in cancer cells including TNBC (Dongoran et al., 2020). In the current research, *CDK6*

and *CDK9* downregulation and *CDKN1A* upregulation occurred in response to lapatinib and BBR treatment through upregulation of cytokines and cytokine receptors, which then led to cell cycle arrest in MDA-MB231 cells. Meanwhile, G0/G1 switch 2 is downregulated after treatment with lapatinib (Fig. 11a). However, FGFR/Akt signaling is

upregulated under the same condition (Fig. 11b). The balance between anti- and pro-proliferative signals mediate dormancy and breast cancer cell growth. Re-differentiation of breast cancer cells into dormancy was previously shown by activation of FGFs and integrins through PI3K/Akt activation (Barrios and Wieder, 2009). CDK6 and DNMT1 downregulation observed in MDA-MB231 cells treated with lapatinib and BBR, suggest that these cells entered dormancy and therefore, cell proliferation is arrested, and instead, the reprogramming of cancer cell signaling leads to angiogenesis and metastasis as well as secretion of pro-inflammatory cytokines as a cellular defense against toxic stress. In agreement with the current findings, CDK6 was reported to be a DNMT, specifically DNMT3B, coregulator. CDK6 binds to DNMTs within the genome (Heller et al., 2020). The lower the CDK6 activity, the lower the accessibility of DNMT3B, suggesting CDK6 plays a regulatory role in DNMT3B activity (Heller et al., 2020). *In vivo* studies have shown that integrin/PI3K/Akt/nuclear factor- κ B signaling pathways have a crucial impact on developing cancer stem cells and the dormancy process, which eventually result in chemoresistance (Qiu et al., 2020).

In addition, we also found that angiogenic biomarkers such as angiogenin/ribonuclease 5 (*ANG/RNASE5*) and angiopoietin-like 4 (*ANGPTL4*) are upregulated in MDA-MB-231 cells treated with lapatinib and BBR (Fig. 11b). Ribonucleases are a family of host proteins secreted in response to stress conditions. For the first time, Hung and his team reported angiogenin/ribonuclease 5 targets RTK EGFR in cancer, and very recently, Hung's team also reported ribonuclease 7 targets RTK ROS1, suggested a new role for ribonucleases, in contrast with ribonucleic anti-inflammatory roles (Liu et al., 2021; Wang et al., 2018). In addition, selective inhibition of angiogenin/ribonuclease 5 suppressed angiogenesis in breast cancer (Li et al., 2020). We observed *ANG*, *RNASE7*, and *RNASE13* were upregulated in TNBC cells after treatment with lapatinib and BBR. *ANG* and *RNASE7* upregulation in lapatinib and BBR treatments suggest they are likely involved in resistance to lapatinib (Fig. 11b). The mechanism is not clear because our results showed EGFR is downregulated in MDA-MB231 after treatment with lapatinib, and *ANG* and *RNASE7* may target other RTKs, required to be elucidated. *RNASE13* is believed to be inactive, and its role is not clear; however, we found *RNASE13* upregulation in lapatinib-treated TNBC cells. Furthermore, *ANGPTL4* is associated with hypoxic condition and angiogenesis as well as poor prognosis in breast cancer (Zhang et al., 2012; Zhao et al., 2020). *ANGPTL4* expression is regulated by RAB11B antisense RNA and promotes angiogenesis in breast cancer (Niu et al., 2020). In agreement with these studies, we found *ANGPTL4* and RAB11B antisense RNA are upregulated after treatment with lapatinib and BBR, suggesting the TNBC cells may have a new opportunity to defend against chemotherapy through activating angiogenesis.

Similarly, the present results revealed that lapatinib and BBR activated Akt through upregulation of *FGFR3*, *TEK*, *FGF9*, and *PGF* as alternative RTKs as well as their ligands in MDA-MB231 cells, along with several genes associated with cell-cell and cell-matrix interactions, such as *ITGA7*, *COL9A3*, *EFNA2/3*, and *TNN* all of which enhance alternative pathways triggering Akt signaling. Notably, KRAS interacts with FGF and vascular endothelial growth factor receptor (VEGF) families to change the behavior of TNBC cells. Another study showed that FGFs, including FGF2 and FGF5, have great potential to force Her2⁺ breast cancer into dormancy and cause resistance to Her2-targeted therapy (Fernández-Nogueira et al., 2020). Moreover, fibroblast-mediated resistance to lapatinib has been shown in breast cancer cells, and sustained activation of PI3K/Akt was reported as a result of FGFR signaling (Zervantonakis et al., 2020). Studies have also shown that cytokines, such as IL-1, inhibit breast cancer cell proliferation and lead to downregulation of several genes associated with tumor progression. Additionally, Akt signaling has been shown to still be activated even if the cell cycle is slowed or arrested (Huang et al., 2017).

As another option for performing angiogenesis, *PGF* expresses placental growth factor (PIGF), which belongs to the VEGF subfamily, is involved in angiogenesis, and promotes re-organization of the cell

cytoskeleton and cellular motility in breast cancer (Malireddy et al., 2013). PIGF is involved in promoting tumor immune escape and metastatic activity through interaction with its main receptor, VEGFR1, and phosphorylation of Akt and p38 MAPK under hypoxic conditions (Albonici et al., 2019; Taylor et al., 2010). In the present study, transcriptomic analysis revealed that lapatinib-activated Akt and p110 alpha regulators were in MDA-MB231 cells. Akt signaling was simultaneously upregulated, while EGFR was downregulated, suggesting Akt may be upregulated by PIGF and FGFs as alternative growth factors in MDA-MB231 cells (Fig. 11c). Activation of Akt signaling under toxic stress may be due to upregulation of *PGF* in treated MDA-MB231 cells. Similarly, PIGF was previously reported to stabilize intermediate filaments, leading to re-arrangement of actin filaments in MDA-MB231 cells which prepares TNBC cells for migration (Taylor et al., 2010). The chemoresistance promoting effect of PIGF has also been reported previously (Albonici et al., 2019; Aoki et al., 2022).

As the main objective of the present research is to study the effects of lapatinib and BBR on PI3K/Akt signaling in resistant TNBC cells, we focused on PI3K signaling; however, our RNA-seq data provides numerous results associated with other signaling pathways. Therefore, we also observed several genes such as *ANGPTL4*, *KITLG* and *FGFRs* as well as genes associated with cancer stemness upregulated in MDA-MB231 after treatment with lapatinib and BBR. Searching the literature showed us PI3K/Akt signaling may play as a central hub in response to chemotherapy affected by various signaling pathways. Other studies also reported the gene profile of MDA-MB231 cells. Bravata et al. (2019) observed upregulated JAK/STAT and Akt signaling pathways in MDA-MB231 cells. They also reported stemness and pluripotency of MDA-MB231 cells through upregulation of *STAT3*, *KRAS*, *FGFR3*, *FGF2*, *PIK3R3*, *KITLG*, *ANGPTL4*, *IL6*, *Akt3* and *Nanog* (Bravata et al., 2019). Upregulation of FGFRs including FGFR3 previously reported in MDA-MB231 cells. Chew et al. (2020) studied FGFR3 signaling in MDA-MB231 cell line and concluded that FGFR3 activity is strongly dependent on FGFR1 and FGFR2 (Chew et al., 2020). They provided a phosphotranscriptomic and functional analysis of MDA-MB231 cells, in which they indicated FGFR1 and FGFR2 are more important than FGFR3. In addition, PD173074 resistant MDA-MB231 cells expresses very low level of FGFR2. Knockdown of FGFR3 did not have any significant effect on MDA-MB231 cells proliferation (Chew et al., 2020). Stress response and anti-oxidant defense pathway has been also reported after treatment with anacardic acid, associated with upregulated PI3K/Akt signaling (Schultz et al., 2018). *ANGPTL4* expression and its association with metastatic growth of TNBC MDA-MB231 cell line was previously reported in several articles. It has been also indicated that chemicals such as diallyl trisulfide and α -lipoic acid decrease *ANGPTL4*, and therefore, decrease metastasis of MDA-MB231 cells (Tripathy et al., 2018; Wei et al., 2017). In addition, Chénais et al. (2020) also showed that *ANGPTL4* is expressed three-time higher in MDA-MB231 cells treated with docosahexaenoic acid indicating cholesterol biosynthesis pathway and ER-stress condition upregulates genes related to angiogenesis and metastasis including *ANGPTL4*, *SERPIN1*, and *MMP11* (Chénais et al., 2020); however, we observed chemoresistant response to lapatinib and BBR in MDA-MB231 cells, which led to *ANGPTL4* upregulation. Furthermore, knockdown of *ANGPTL4* in MDA-MB231 cells cultured astrocyte-conditioned media reduced metastasis in brain. *ANGPTL4* expressed in MDA-MB231 is not only involved in metastasis, but the transforming growth factor-beta 2 (TGF- β 2) produced by astrocytes also upregulates *ANGPTL4* in MDA-MB231 cells (Gong et al., 2019). MDA-MB231 cells may also show resistance to immuno cell-mediated cytotoxicity. Doxorubicin sensitizes resistant MDA-MB231 cell line to immuno cell-mediated cytotoxicity (Inao et al., 2019). Inao et al. (2019) observed senescent cancer cells promote tumor formation by producing cytokines and growth factors (Inao et al., 2019). Additionally, Li et al. (2017) observed that low-dose irradiation enhances proliferation of MDA-MB231 cells. They found radiation accelerated entry to S phase of MDA-MB231 cell cycle through upregulation of CDK6

and CDK4 in response to accumulation of mutated p53 (Li et al., 2017). Accordingly, resistance of MDA-MB231 cells to chemotherapy, immunotherapy, and radiotherapy reported in some research may be associated with senescence, and hence, the higher number of cell passage may decrease sensitivity of MDA-MB231 cells to therapy (Inao et al., 2019; Jabbarzadeh Kaboli and Ling, 2020; Li et al., 2017; van der Noord et al., 2019).

The present study is the first pharmacotranscriptomic report of lapatinib and BBR causing overactivation of Akt in chemoresistant MDA-MB231 TNBC. In addition, our qPCR data showed PIK3CA and PIK3R1 are overexpressed in MDA-MB231 cells after treatment with lapatinib and BBR. These findings show that lapatinib and BBR may upregulate KRAS and alternative growth factor receptors in TNBC in an EGFR-independent manner. Although the data is promising, some limitations are present including lacking lapatinib-treated TNBC patients. If we could have access to clinical data obtained from TNBC patients treated with lapatinib or other TKIs, we could observe acquired resistance to TKIs in some cases, and further whole genome RNA-seq analysis could help us in addressing the molecular mechanism of drug resistance in TNBC. Furthermore, gene expression does not mean production of activated protein, and therefore, functional study is required; however, transcriptomic data provide great source for future research design. Further studies are needed to reproduce this data to determine the toxicity profiles and cellular mechanisms underlying the enhanced therapeutic efficacy of lapatinib and BBR. Meanwhile, future pharmacogenetics and pharmacoepigenetics studies will open new opportunities for the development of anti-angiogenic drugs. As such, systematized *in vivo* and *in vitro* protocols and clinical studies with larger samples sizes are needed to fully investigate the therapeutic efficacy of lapatinib and BBR in chemoresistant TNBC patients.

5. Conclusions

After treating MDA-MB231 cells with lapatinib and BBR alone and in combination, it was concluded that KRAS overactivation bypasses EGFR sensitivity and upregulates alternative growth factors, such as PlGF and FGFs, which may be an alternative way to upregulate Akt signaling under toxic stress resultant from high concentrations of lapatinib and BBR. Moreover, the present study showed the mechanism for chemoresistance in TNBC cells may be through RTK upregulation, angiogenesis activation, and reprogrammed cell-cell interactions and therefore, alternative TKIs and angiogenesis inhibitors as well as KRAS inhibitors are predicted to be effective alternative treatment combinations in Akt-targeted therapy whenever EGFR/Her2-targeted therapy is not effective for TNBC. The products of genes listed in the present research can also be considered biomarkers for encountering chemoresistance to lapatinib in TNBC; however, the mechanisms of resistance to Akt inhibitors require more study.

Funding

This work was supported by Southwest Medical University (SWMU) grants 05/00040129 and 2019ZQN001 awarded to PJK. This work was also supported by National Natural Science Foundation of China (No. 81972643, No. 82172962), Sichuan Science and Technology Project (2021YJ0201), Luxian People's Government and Southwest Medical University Scientific and Technological Achievements Transfer and Transformation Strategic Cooperation Project (2019LXXNYKD-07) and Science and Technology Program of Luzhou, China (No. 21CGZHPT0001).

Declaration of interests

Zhangang Xiao reports financial support was provided by Southwest Medical University and National Natural Science Foundation of China. Parham Jabbarzadeh Kaboli reports financial support was provided by

Southwest Medical University.

CRediT authorship contribution statement

Parham Jabbarzadeh Kaboli: Supervision, Funding acquisition, Writing – original draft. **Shuang Luo:** Formal analysis, Investigation. **Yao Chen:** Formal analysis, Investigation. **Masume Jomhori:** Visualization, Data curation, Formal Analysis. **Saber Imani:** Formal analysis, Writing – review & editing. **Shixin Xiang:** Investigation, Visualization. **Zhigui Wu:** Methodology. **Mingxing Li:** Methodology. **Jing Shen:** Data curation. **Yueshui Zhao:** Writing – review & editing. **Xu Wu:** Writing – review & editing. **Chi Hin Cho:** Writing – review & editing. **Zhangang Xiao:** Supervision, Funding acquisition.

Declaration of Competing Interest

The authors declare that they have no known competing financial interests or personal relationships that could have appeared to influence the work reported in this paper.

Appendix A. Supplementary material

Supplementary data to this article can be found online at <https://doi.org/10.1016/j.gene.2021.146171>.

References

- Albonici, L., Giganti, M.G., Modesti, A., Manzari, V., Bei, R., 2019. Multifaceted role of the placental growth factor (PlGF) in the antitumor immune response and cancer progression. *Int. J. Mol. Sci.* 20 (12), 2970. <https://doi.org/10.3390/ijms20122970>.
- Aoki, S., Inoue, K., Klein, S., Halvorsen, S., Chen, J., Matsui, A., Nikmaneshi, M.R., Kitahara, S., Hato, T., Chen, X., Kawakubo, K., Nia, H.T., Chen, I., Schanne, D.H., Mamessier, E., Shigeta, K., Kikuchi, H., Ramjiawan, R.R., Schmidt, T.C.E., Iwasaki, M., Yau, T., Hong, T.S., Quaas, A., Plum, P.S., Dima, S., Popescu, I., Bardeesy, N., Munn, L.L., Borad, M.J., Sassi, S., Jain, R.K., Zhu, A.X., Duda, D.G., 2022. Placental growth factor promotes tumour desmoplasia and treatment resistance in intrahepatic cholangiocarcinoma. *Gut* 71 (1), 185–193. <https://doi.org/10.1136/gutjnl-2020-322493>.
- Barrios, J., Wieder, R., 2009. Dual FGF-2 and integrin alpha5beta1 signaling mediate GRAF-induced RhoA inactivation in a model of breast cancer dormancy. *Can. Microenviron. Off. J. Int. Cancer Microenviron. Soc.* 2, 33–47. <https://doi.org/10.1007/s12307-009-0019-6>.
- Beniey, Michèle, et al., 2019. Translating the role of PARP inhibitors in triple-negative breast cancer. *Oncoscience* 6 (1–2), 287–288. <https://doi.org/10.18632/oncoscience.474>.
- Bourdeau, V., Ferbeyre, G., 2016. CDK4-CDK6 inhibitors induce autophagy-mediated degradation of DNMT1 and facilitate the senescence antitumor response. *Autophagy* 12 (10), 1965–1966. <https://doi.org/10.1080/15548627.2016.1214779>.
- Bravata, V., Cammarata, F.P., Minafra, L., Musso, R., Pucci, G., Spada, M., Fazio, I., Russo, G., Forte, G.L., 2019. Gene expression profiles induced by high-dose ionizing radiation in MDA-MB-231 triple-negative breast cancer cell line. *Can. Gen. Proteom.* 16, 257–266. <https://doi.org/10.21873/cgp.20130>.
- Chénais, B., Cornec, M., Dumont, S., Marchand, J., Blanckaert, V., 2020. Transcriptomic response of breast cancer cells MDA-MB-231 to docosahexaenoic acid: downregulation of lipid and cholesterol metabolism genes and upregulation of genes of the pro-apoptotic ER-stress pathway. *Int. J. Environ. Res. Public Health* 17 (10), 3746. <https://doi.org/10.3390/ijerph17103746>.
- Chew, N.J., Nguyen, E.V., Su, S.-P., Novy, K., Chan, H.C., Nguyen, L.K., Luu, J., Simpson, K.J., Lee, R.S., Daly, R.J., 2020. FGFR3 signaling and function in triple negative breast cancer. *Cell Commun. Signal.* 18, 13. <https://doi.org/10.1186/s12964-019-0486-4>.
- Costa, R., Shah, A.N., Santa-Maria, C.A., Cruz, M.R., Mahalingam, D., Carneiro, B.A., Chae, Y.K., Cristofanilli, M., Gradishar, W.J., Giles, F.J., 2017. Targeting Epidermal Growth Factor Receptor in triple negative breast cancer: new discoveries and practical insights for drug development. *Cancer Treat. Rev.* 53, 111–119. <https://doi.org/10.1016/j.ctrv.2016.12.010>.
- Dongoran, R.A., Wang, K.-H., Lin, T.-J., Yuan, T.-C., Liu, C.-H., 2020. Anti-proliferative effect of statins is mediated by DNMT1 inhibition and p21 expression in OSCC cells. *Cancers* 12 (8), 2084. <https://doi.org/10.3390/cancers12082084>.
- Fernández-Nogueira, P., Mancino, M., Fuster, G., López-Plana, A., Jauregui, P., Almendro, V., Enreig, E., Menéndez, S., Rojo, F., Noguera-Castells, A., Bill, A., Gauthier, L.A., Serrano, L., Recalde-Percaz, L., Moragas, N., Alonso, R., Ametller, E., Rovira, A., Lluch, A., Albanell, J., Gascon, P., Bragado, P., 2020. Tumor-associated fibroblasts promote HER2-targeted therapy resistance through FGFR2 activation. *Clin. Can. Res.* 26 (6), 1432–1448. <https://doi.org/10.1158/1078-0432.CCR-19-0353>.

- Gohr, K., Hamacher, A., Engelke, L.H., Kassack, M.U., 2017. Inhibition of PI3K/Akt/mTOR overcomes cisplatin resistance in the triple negative breast cancer cell line HCC38. *BMC Can.* 17, 711. <https://doi.org/10.1186/s12885-017-3695-5>.
- Gong, X., Hou, Z., Endsley, M.P., Gronseth, E.I., Rarick, K.R., Jorns, J.M., Yang, Q., Du, Z., Yan, K., Bordas, M.L., Gershan, J., Deepak, P., Geethadevi, A., Chaluvally-Raghavan, P., Fan, Y., Harder, D.R., Ramchandran, R., Wang, L., 2019. Interaction of tumor cells and astrocytes promotes breast cancer brain metastases through TGF- β /ANGPTL4 axes. *NPJ Precis. Oncol.* 3, 24. <https://doi.org/10.1038/s41698-019-0094-1>.
- Heller, G., Nebenfuhr, S., Bellutti, F., Ünal, H., Zojer, M., Scheiblecker, L., Sexl, V., Kollmann, K., 2020. The Effect of CDK6 Expression on DNA Methylation and DNMT3B. *Regulation.* 23 (10), 101602. <https://doi.org/10.1016/j.isci.2020.101602>.
- Huang, J., Woods, P., Normolle, D., Goff, J.P., Benos, P.V., Stehle, C.J., Steinman, R.A., 2017. Downregulation of estrogen receptor and modulation of growth of breast cancer cell lines mediated by paracrine stromal cell signals. *Breast Can. Res. Treat.* 161 (2), 229–243. <https://doi.org/10.1007/s10549-016-4052-0>.
- Inao, T., Kotani, H., Iida, Y., Kartika, I.D., Okimoto, T., Tanino, R., Shiba, E., Harada, M., 2019. Different sensitivities of senescent breast cancer cells to immune cell-mediated cytotoxicity. *Can. Sci.* 110 (9), 2690–2699. <https://doi.org/10.1111/cas.14116>.
- Jabbarzadeh Kaboli, Parham, et al., 2021. Chemoresistance in breast cancer: PI3K/Akt pathway inhibitors vs the current chemotherapy. *American Journal of Cancer Research* 11 (10), 5155–5183.
- Jabbarzadeh Kaboli, P., Leong, M.-Y., Ismail, P., Ling, K.-H., 2019. Antitumor effects of berberine against EGFR, ERK1/2, P38 and AKT in MDA-MB231 and MCF-7 breast cancer cells using molecular modelling and in vitro study. *Pharmacol. Rep.* 71 (1), 13–23. <https://doi.org/10.1016/j.pharep.2018.07.005>.
- Kaboli, P.J., Ling, K.-H., 2020. Lapatinib as a dual tyrosine kinase inhibitor unexpectedly activates Akt in MDA-MB-231 triple-negative breast cancer cells. *Lett. Drug Des. Discov.* 17 (8), 1060–1063.
- Jabbarzadeh Kaboli, P., Rahmat, A., Ismail, P., Ling, K.-H., 2014. Targets and mechanisms of berberine, a natural drug with potential to treat cancer with special focus on breast cancer. *Eur. J. Pharmacol.* 740, 584–595. <https://doi.org/10.1016/j.ejphar.2014.06.025>.
- Jabbarzadeh Kaboli, P., Salimian, F., Aghapour, S., Xiang, S., Zhao, Q., Li, M., Wu, X.u., Du, F., Zhao, Y., Shen, J., Cho, C.H., Xiao, Z., 2020. Akt-targeted therapy as a promising strategy to overcome drug resistance in breast cancer – a comprehensive review from chemotherapy to immunotherapy. *Pharmacol. Res.* 156, 104806. <https://doi.org/10.1016/j.phrs.2020.104806>.
- Kaboli, P.J., Bazrafkan, M., Ismail, P., Ling, K.-H., 2017. Molecular modelling of berberine derivatives as inhibitors of human smoothed receptor and hedgehog signalling pathway using a newly developed algorithm on anti-cancer drugs. *Recent Pat. Anticancer. Drug Discov.* 12, 384–400. <https://doi.org/10.2174/1574892812666170929131247>.
- Li, B., Dewey, C.N., 2011. RSEM: accurate transcript quantification from RNA-Seq data with or without a reference genome. *BMC Bioinf.* 12, 323. <https://doi.org/10.1186/1471-2105-12-323>.
- Li, S.-Y., Liang, X.-Y., Li, H.-J., Li, W., Zhou, L., Chen, H.-Q., Ye, S.-G., Yu, D.-H., Cui, J.-W., 2017. Low-dose irradiation promotes proliferation of the human breast cancer MDA-MB-231 cells through accumulation of mutant P53. *Int. J. Oncol.* 50, 290–296. <https://doi.org/10.3892/ijo.2016.3795>.
- Li, Y., Qu, X., Cao, B., Yang, T., Bao, Q., Yue, H., Zhang, L., Zhang, G., Wang, L., Qiu, P., Zhou, N., Yang, M., Mao, C., 2020. Selectively suppressing tumor angiogenesis for targeted breast cancer therapy by genetically engineered phage. *Adv. Mater.* 32 (29), 2001260. <https://doi.org/10.1002/adma.202001260>.
- Liu, C., Zha, Z., Zhou, C., Chen, Y., Xia, W., Wang, Y.-N., Lee, H.-H., Yin, Y., Yan, M., Chang, C.-W., Chan, L.-C., Qiu, Y., Li, H., Li, C.-W., Hsu, J.-M., Hsu, J.L., Wang, S.-C., Ren, N., Hung, M.-C., 2021. Ribonuclease 7-driven activation of ROS1 is a potential therapeutic target in hepatocellular carcinoma. *J. Hepatol.* 74 (4), 907–918. <https://doi.org/10.1016/j.jhep.2020.09.030>.
- Malireddy, S., Lawson, C., Steinhour, E., Hart, J., Kotha, S.R., Patel, R.B., Zhao, L., Wilkins, J.R., Marsh, C.B., Magalag, U.J., Romberger, D., Wewers, M.D., Parinandi, N.L., 2013. Airborne agricultural particulate matter induces inflammatory cytokine secretion by respiratory epithelial cells: mechanisms of regulation by eicosanoid lipid signal mediators. *Indian J. Biochem. Biophys.* 50, 387–401.
- McLaughlin, R.P., He, J., van derNoord, V.E., Redel, J., Foekens, J.A., Martens, J.W.M., Smid, M., Zhang, Y., van deWater, B., 2019. A kinase inhibitor screen identifies a dual cdc7/CDK9 inhibitor to sensitize triple-negative breast cancer to EGFR-targeted therapy. *Breast Cancer Res.* 21, 77. <https://doi.org/10.1186/s13058-019-1161-9>.
- Nitulescu, G.M., Margina, D., Juzenas, P., Peng, Q., Oлару, O.T., Saloustros, E., Fenga, C., Spandidos, D.A., Libra, M., Tzatsakis, A.M., 2016. Akt inhibitors in cancer treatment: The long journey from drug discovery to clinical use (Review). *Int. J. Oncol.* 48, 869–885. <https://doi.org/10.3892/ijo.2015.3306>.
- Niu, Y., Bao, L., Chen, Y., Wang, C., Luo, M., Zhang, B.o., Zhou, M.i., Wang, J.E., Fang, Y. V., Kumar, A., Xing, C., Wang, Y., Luo, W., 2020. HIF2-induced long noncoding RNA RAB11B-AS1 promotes hypoxia-mediated angiogenesis and breast cancer metastasis. *Cancer Res.* 80 (5), 964–975. <https://doi.org/10.1158/0008-5472.CAN-19-1532>.
- Qiu, Y., Qiu, S., Deng, L., Nie, L., Gong, L., Liao, X., Zheng, X., Jin, K., Li, J., Tu, X., Liu, L., Liu, Z., Bao, Y., Ai, J., Lin, T., Yang, L.u., Wei, Q., 2020. Biomaterial 3D collagen I gel culture model: A novel approach to investigate tumorigenesis and dormancy of bladder cancer cells induced by tumor microenvironment. *Biomaterials* 256, 120217. <https://doi.org/10.1016/j.biomaterials.2020.120217>.
- Robinson, M.D., McCarthy, D.J., Smyth, G.K., 2010. edgeR: a Bioconductor package for differential expression analysis of digital gene expression data. *Bioinformatics* 26 (1), 139–140. <https://doi.org/10.1093/bioinformatics/btp16>.
- Ruprecht, B., Zaal, E.A., Zecha, J., Wu, W., Berkers, C.R., Kuster, B., Lemeer, S., 2017. Lapatinib resistance in breast cancer cells is accompanied by phosphorylation-mediated reprogramming of glycolysis. *Cancer Res.* 77 (8), 1842–1853. <https://doi.org/10.1158/0008-5472.CAN-16-2976>.
- Saatci, O., Kaymak, A., Raza, U., Ersan, P.G., Akbulut, O., Banister, C.E., Sikirzhyski, V., Tokat, U.M., Aykut, G., Ansari, S.A., Dogan, H.T., Dogan, M., Jandaghi, P., Isik, A., Gundogdu, F., Kosemehmetoglu, K., Dizdar, O., Aksoy, S., Akyol, A., Uner, A., Buckhaults, P.J., Riazalhosseini, Y., Sahin, O., 2020. Targeting lysyl oxidase (LOX) overcomes chemotherapy resistance in triple negative breast cancer. *Nat. Commun.* 11, 2416. <https://doi.org/10.1038/s41467-020-16199-4>.
- Saleh, R., Taha, R.Z., Sasidharan Nair, V., Alajez, N.M., Elkord, E., 2019. PD-L1 blockade by atezolizumab downregulates signaling pathways associated with tumor growth, metastasis, and hypoxia in human triple negative breast cancer. *Cancers* 11 (8), 1050. <https://doi.org/10.3390/cancers11081050>.
- Schultz, D.J., Krishna, A., Vittitow, S.L., Alizadeh-Rad, N., Muluhngwi, P., Rouchka, E.C., Klinge, C.M., 2018. Transcriptomic response of breast cancer cells to anacardic acid. *Sci. Rep.* 8, 8063. <https://doi.org/10.1038/s41598-018-26429-x>.
- Shen, S., Park, J.W., Huang, J., Dittmar, K.A., Lu, Z.-X., Zhou, Q., Carstens, R.P., Xing, Y. i., 2012. MATS: a Bayesian framework for flexible detection of differential alternative splicing from RNA-Seq data. *Nucleic Acids Res.* 40 (8), e61. <https://doi.org/10.1093/nar/gkr1291>.
- Taylor, A.P., Leon, E., Goldenberg, D.M., 2010. Placental growth factor (PlGF) enhances breast cancer cell motility by mobilising ERK1/2 phosphorylation and cytoskeletal rearrangement. *Br. J. Cancer* 103 (1), 82–89. <https://doi.org/10.1038/sj.bjc.6605746>.
- Thike, A.A., Cheok, P.Y., Jara-Lazaro, A.R., Tan, B., Tan, P., Tan, P.H., 2010. Triple-negative breast cancer: clinicopathological characteristics and relationship with basal-like breast cancer. *Mod Pathol* 23 (1), 123–133.
- Trapnell, C., Pachter, L., Salzberg, S.L., 2009. TopHat: discovering splice junctions with RNA-Seq. *Bioinformatics* 25, 1105–1111. <https://doi.org/10.1093/bioinformatics/btp120>.
- Tripathy, J., Tripathy, A., Thangaraju, M., Suar, M., Elangovan, S., 2018. α -Lipoic acid inhibits the migration and invasion of breast cancer cells through inhibition of TGF β signaling. *Life Sci.* 207, 15–22. <https://doi.org/10.1016/j.lfs.2018.05.039>.
- van derNoord, V.E., McLaughlin, R.P., Smid, M., Foekens, J.A., Martens, J.W.M., Zhang, Y., van deWater, B., 2019. An increased cell cycle gene network determines MEK and Akt inhibitor double resistance in triple-negative breast cancer. *Sci. Rep.* 9, 13308. <https://doi.org/10.1038/s41598-019-49809-3>.
- Wang, Y.-N., Lee, H.-H., Chou, C.-K., Yang, W.-H., Wei, Y., Chen, C.-T., Yao, J., Hsu, J.L., Zhu, C., Ying, H., Ye, Y., Wang, W.-J., Lim, S.-O., Xia, W., Ko, H.-W., Liu, X., Liu, C.-G., Wu, X., Wang, H., Li, D., Prakash, L.R., Katz, M.H., Kang, Y., Kim, M., Fleming, J. B., Fogelman, D., Javle, M., Maitra, A., Hung, M.-C., 2018. Angiogenin/ribonuclease 5 is an EGFR ligand and a serum biomarker for erlotinib sensitivity in pancreatic cancer. *Cancer Cell* 33 (4), 752–769.e8. <https://doi.org/10.1016/j.ccell.2018.02.012>.
- Wei, Z., Shan, Y., Tao, L.i., Liu, Y., Zhu, Z., Liu, Z., Wu, Y., Chen, W., Wang, A., Lu, Y., 2017. Diallyl trisulfides, a natural histone deacetylase inhibitor, attenuate HIF-1 α synthesis, and decreases breast cancer metastasis. *Mol. Carcinog.* 56 (10), 2317–2331. <https://doi.org/10.1002/mc.22686>.
- Werfel, T.A., Wang, S., Jackson, M.A., Kavanagh, T.E., Joly, M.M., Lee, L.H., Hicks, D.J., Sanchez, V., Ericsson, P.G., Kilchrist, K.V., Dimobi, S.C., Saret, S.M., Brantley-Sieders, D.M., Cook, R.S., Duvall, C.L., 2018. Selective mTORC2 inhibitor therapeutically blocks breast cancer cell growth and survival. *Cancer Res.* 78 (7), 1845–1858. <https://doi.org/10.1158/0008-5472.CAN-17-2388>.
- Xie, C., Mao, X., Huang, J., Ding, Y., Wu, J., Dong, S., Kong, L., Gao, G., Li, C.-Y., Wei, L., 2011. KOBAS 2.0: a web server for annotation and identification of enriched pathways and diseases. *Nucleic Acids Res.* 39, W316–W322. <https://doi.org/10.1093/nar/gkr483>.
- Young, A., Lou, D., McCormick, F., 2013. Oncogenic and wild-type Ras play divergent roles in the regulation of mitogen-activated protein kinase signaling. *Cancer Discov.* 3 (1), 112–123. <https://doi.org/10.1158/2159-8290.CD-12-0231>.
- Zervantonakis, I.K., Poskus, M.D., Scott, A.L., Seflors, L.M., Lin, J.-R., Dillon, D.A., Pathania, S., Sorger, P.K., Mills, G.B., Brugge, J.S., 2020. Fibroblast-tumor cell signaling limits HER2 kinase therapy response via activation of MTOR and antiapoptotic pathways. *Proc. Natl. Acad. Sci. U. S. A.* 117 (28), 16500–16508. <https://doi.org/10.1073/pnas.2000648117>.
- Zhang, H., Pandey, S., Travers, M., Sun, H., Morton, G., Madzo, J., Chung, W., Khowsathit, J., Perez-Leal, O., Barrero, C.A., Merali, C., Okamoto, Y., Sato, T., Pan, J., Garriga, J., Bhanu, N.V., Simithy, J., Patel, B., Huang, J., Raynal, N.-M., Garcia, B.A., Jacobson, M.A., Kadoch, C., Merali, S., Zhang, Y.i., Childers, W., Abou-Gharbia, M., Karanicolos, J., Baylin, S.B., Zahnow, C.A., Jelinek, J., Graña, X., Issa, J.-P., 2018. Targeting CDK9 reactivates epigenetically silenced genes in cancer. *Cell* 175 (5), 1244–1258.e26. <https://doi.org/10.1016/j.cell.2018.09.051>.
- Zhang, H., Wong, C.C.L., Wei, H., Gilkes, D.M., Korangath, P., Chaturvedi, P., Schito, L., Chen, J., Krishnamachary, B., Winnard, P.T., Raman, V., Zhen, L., Mitzner, W.A., Sukumar, S., Semenza, G.L., 2012. HIF-1-dependent expression of angiopoietin-like 4 and L1CAM mediates vascular metastasis of hypoxic breast cancer cells to the lungs. *Oncogene* 31 (14), 1757–1770. <https://doi.org/10.1038/onc.2011.365>.
- Zhao, J., Liu, J., Wu, N., Zhang, H., Zhang, S., Li, L., Wang, M., 2020. ANGPTL4 overexpression is associated with progression and poor prognosis in breast cancer. *Oncol. Lett.* 20 (3), 2499–2505. <https://doi.org/10.3892/ol.2020.11768>.
- Zhao, Y., Zhao, Q., Kaboli, P.J., Shen, J., Li, M., Wu, X.u., Yin, J., Zhang, H., Wu, Y., Lin, L., Zhang, L., Wan, L., Wen, Q., Li, X., Cho, C.H., Yi, T., Li, J., Xiao, Z., 2019. m1A Regulated Genes Modulate PI3K/AKT/mTOR and ErbB Pathways in Gastrointestinal Cancer. *Transl. Oncol.* 12 (10), 1323–1333.